APPENDIX A: AERIAL PHOTOS

A.1. June 2006

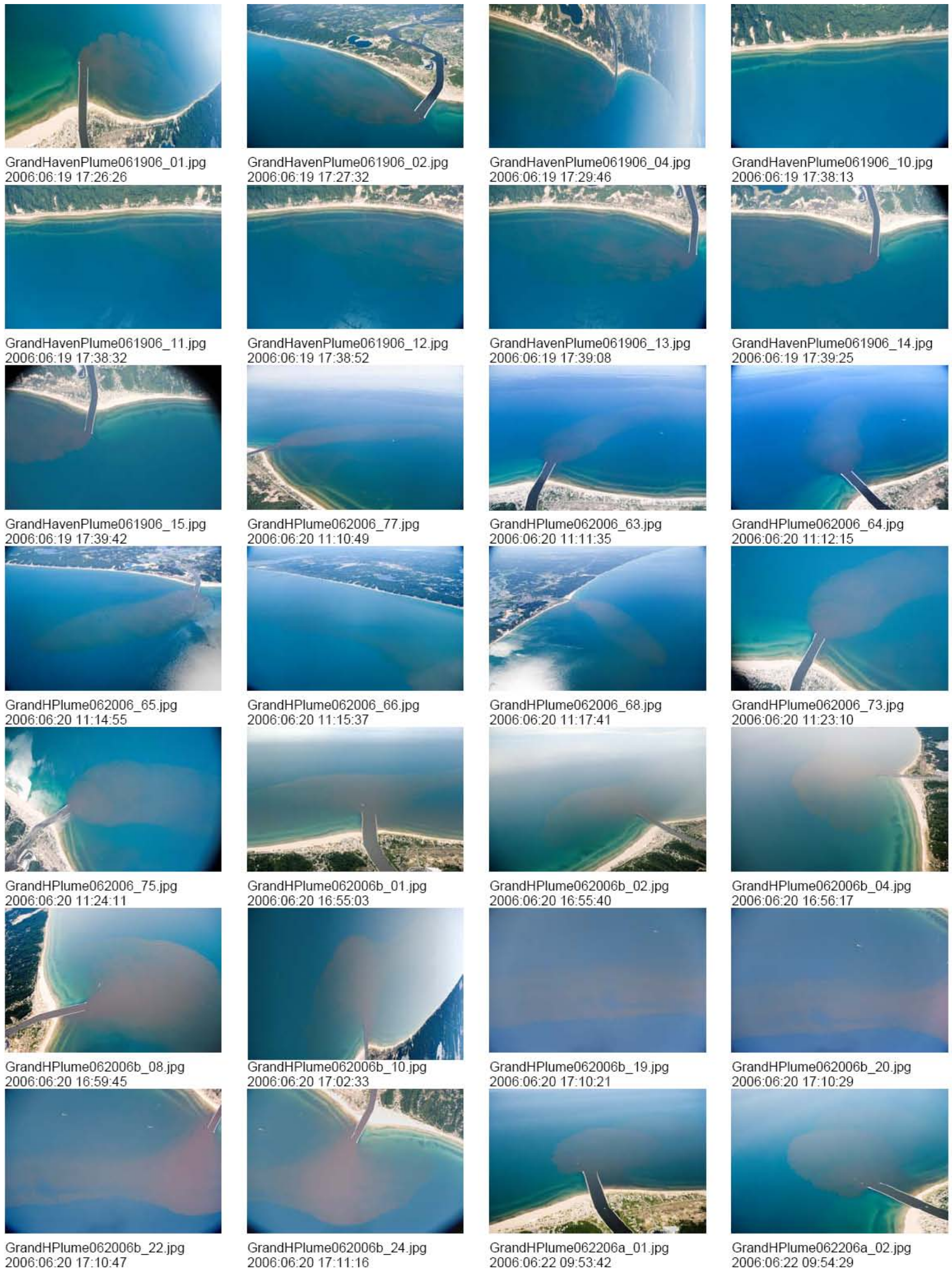

Figure A.1. Aerial pictures of the Grand Haven Plume from June 19, 2006 17:26:26 EDT to June 22, 2006 9:54:29 EDT.

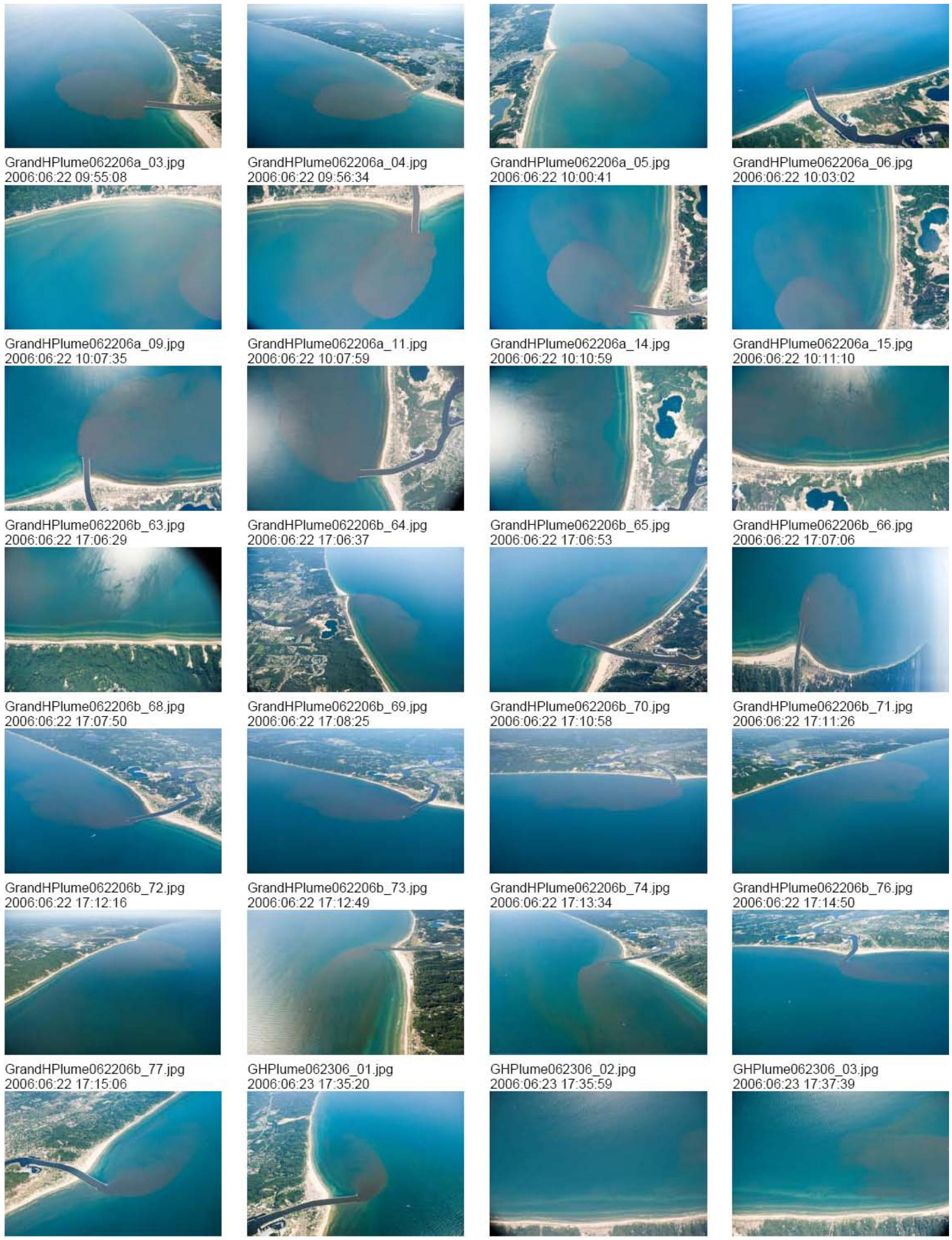

Figure A.2. Aerial pictures of the Grand Haven Plume from June 22, 2006 9:55:08 EDT to June 23, 2006 17:44:53 EDT.

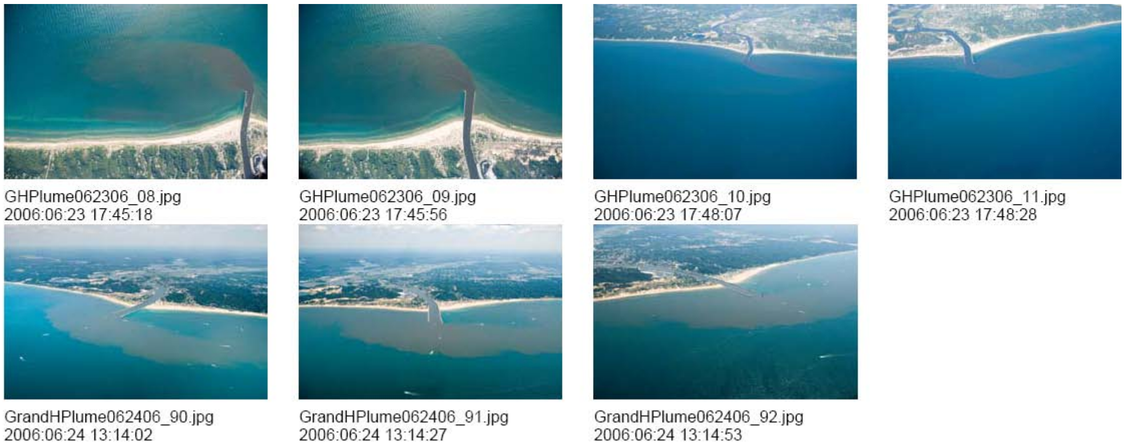

Figure A.3. Aerial pictures of the Grand Haven Plume from June 22, 2006 from 9:55:08 EDT to June 23, 2006 17:44:53 EDT.

A.2. August 2006

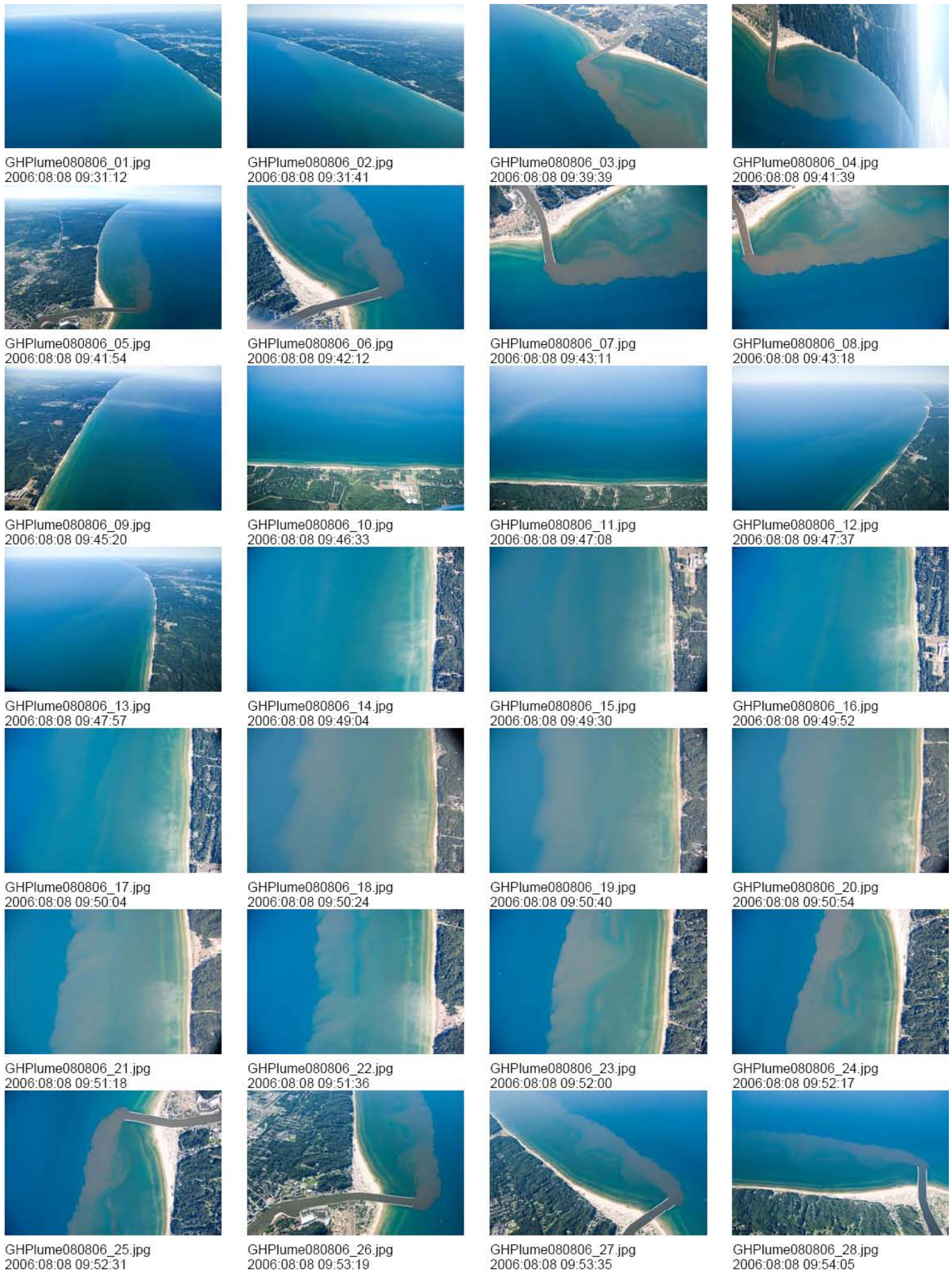

Figure A.4. Aerial pictures of the Grand Haven Plume on August 8, 2006 from 09:13:12 to 09:54:05 EDT.

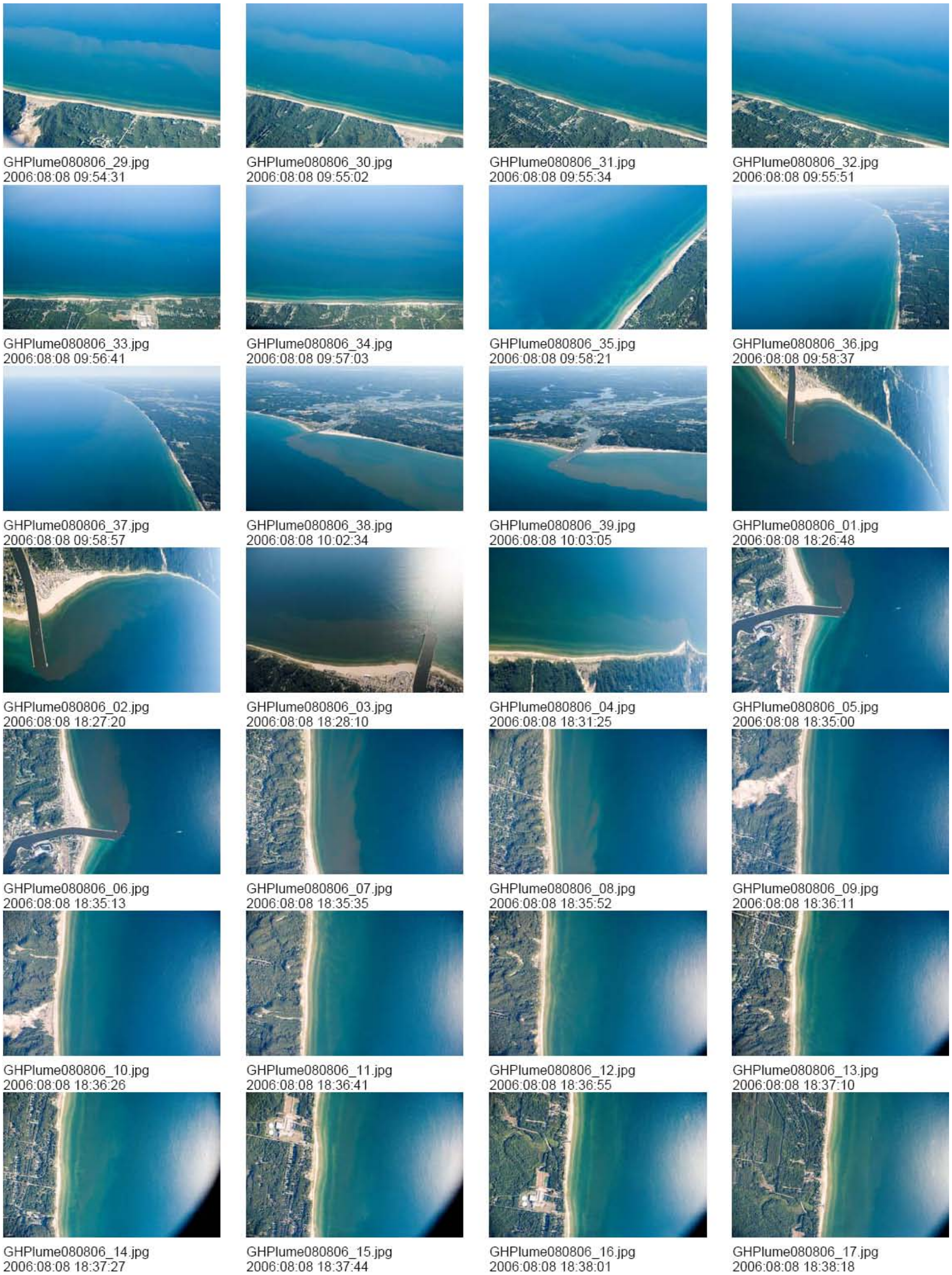

Figure A.5. Aerial pictures of the Grand Haven Plume on August 8, 2006 from 09:54:31 to 18:38:18 EDT.

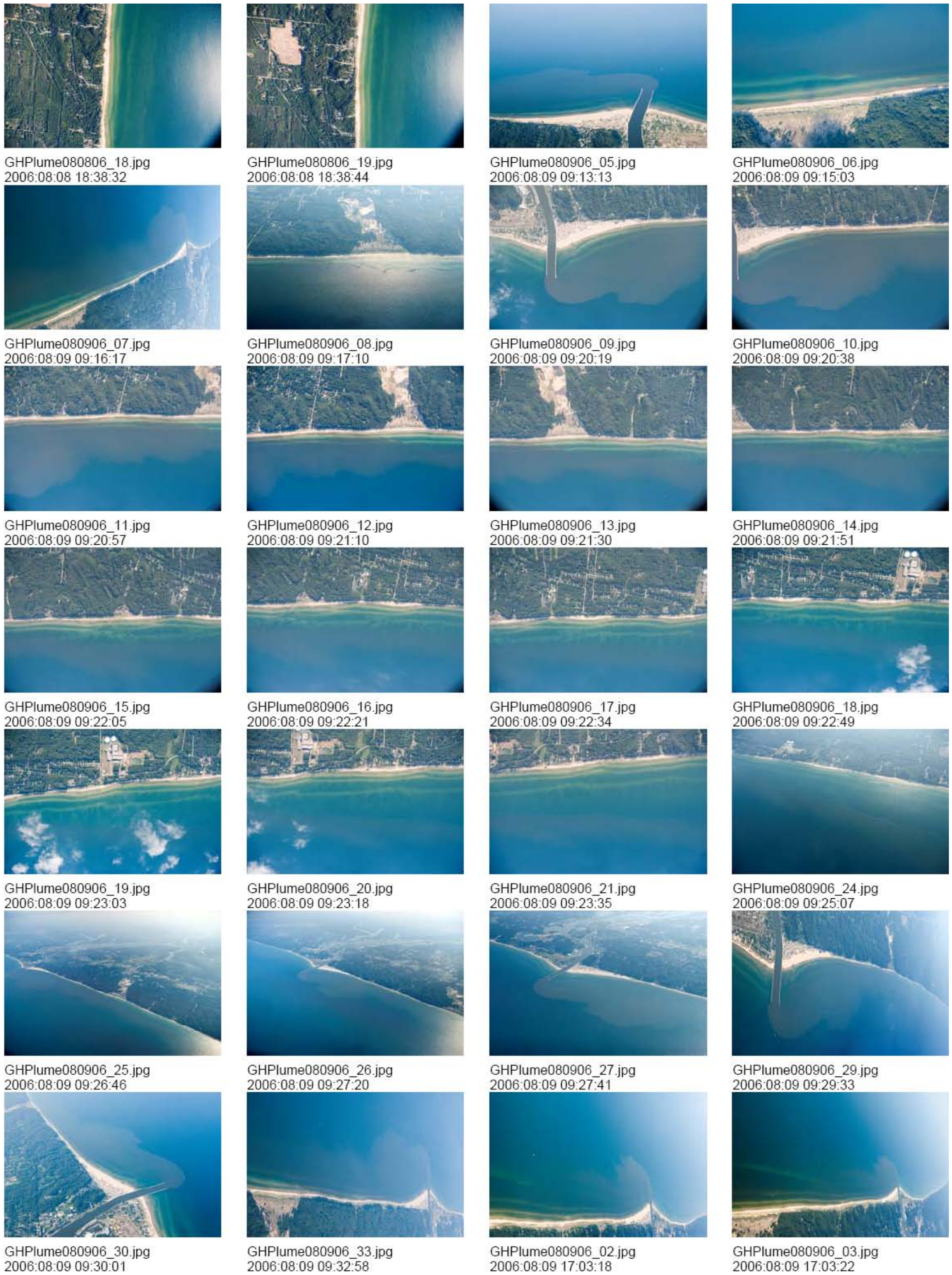

Figure A.6. Aerial pictures of the Grand Haven Plume on August 9, 2006 from 18:38:22 to 17:03:22 EDT.

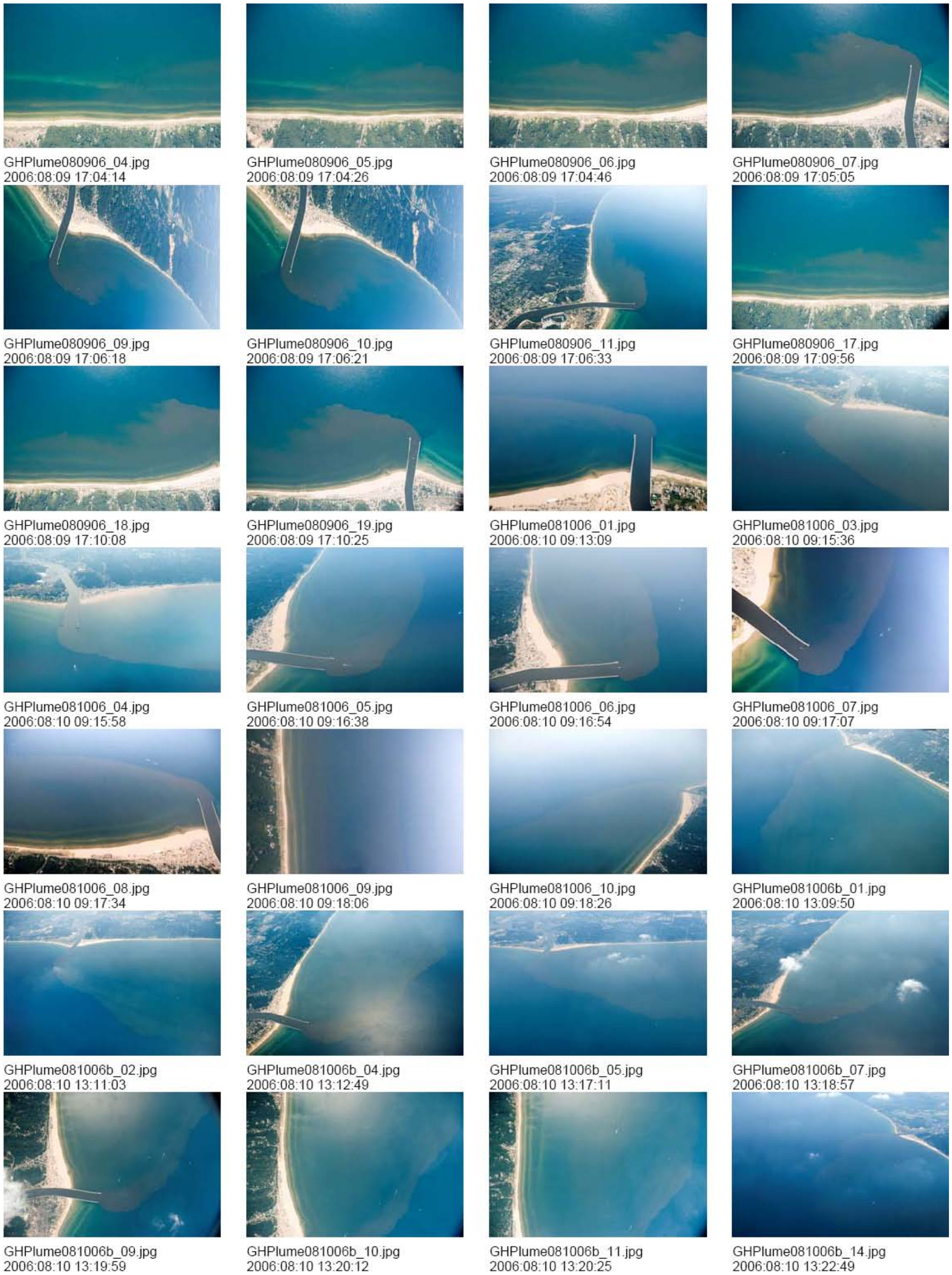

Figure A.7. Aerial pictures of the Grand Haven Plume on August 9, 2006 from 17:4:14 to 13:22:49 EDT.

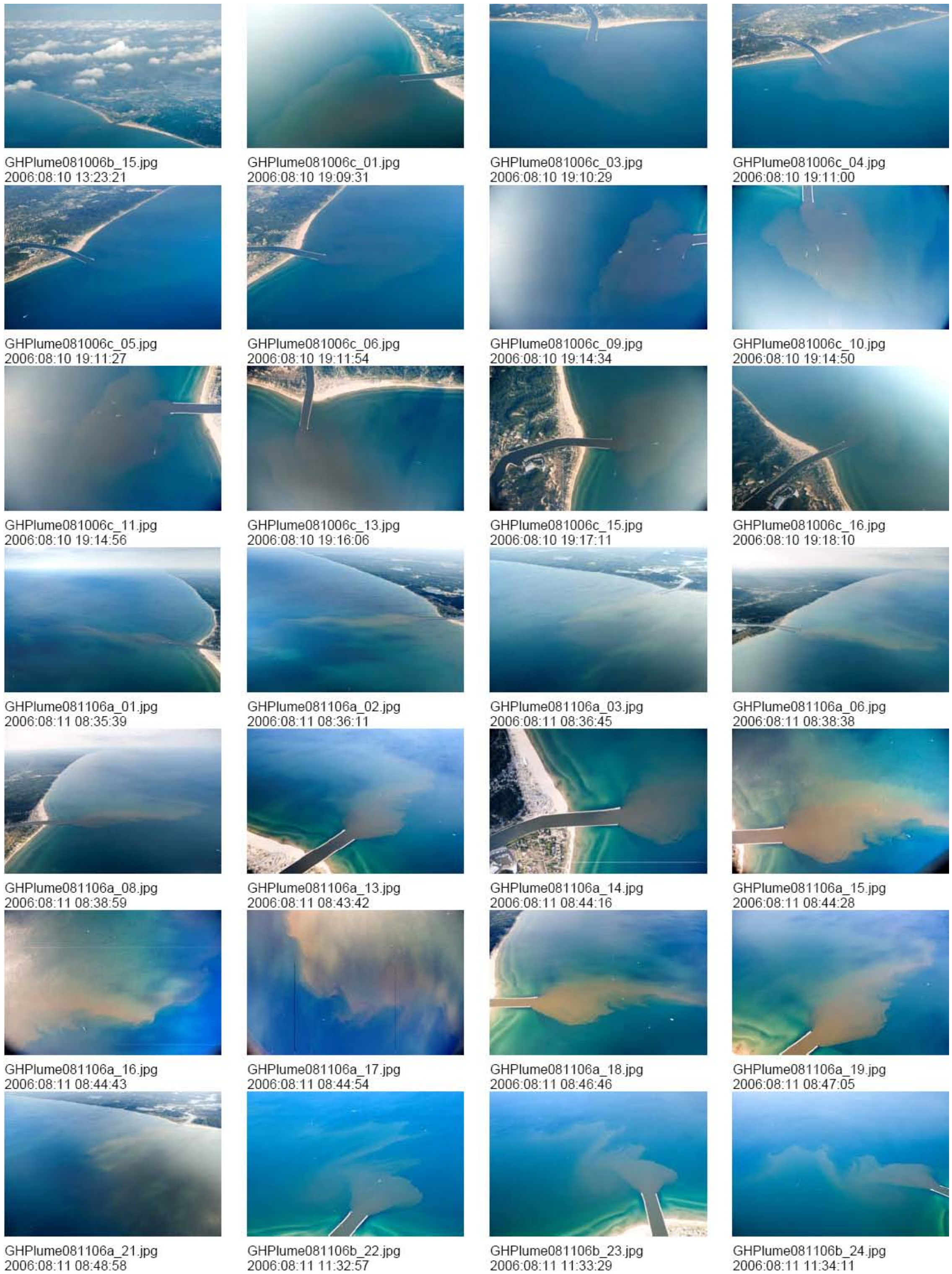

Figure A.8. Aerial pictures of the Grand Haven Plume on August 10, 2006 from 13:23:21 to 11:34:11 EDT.

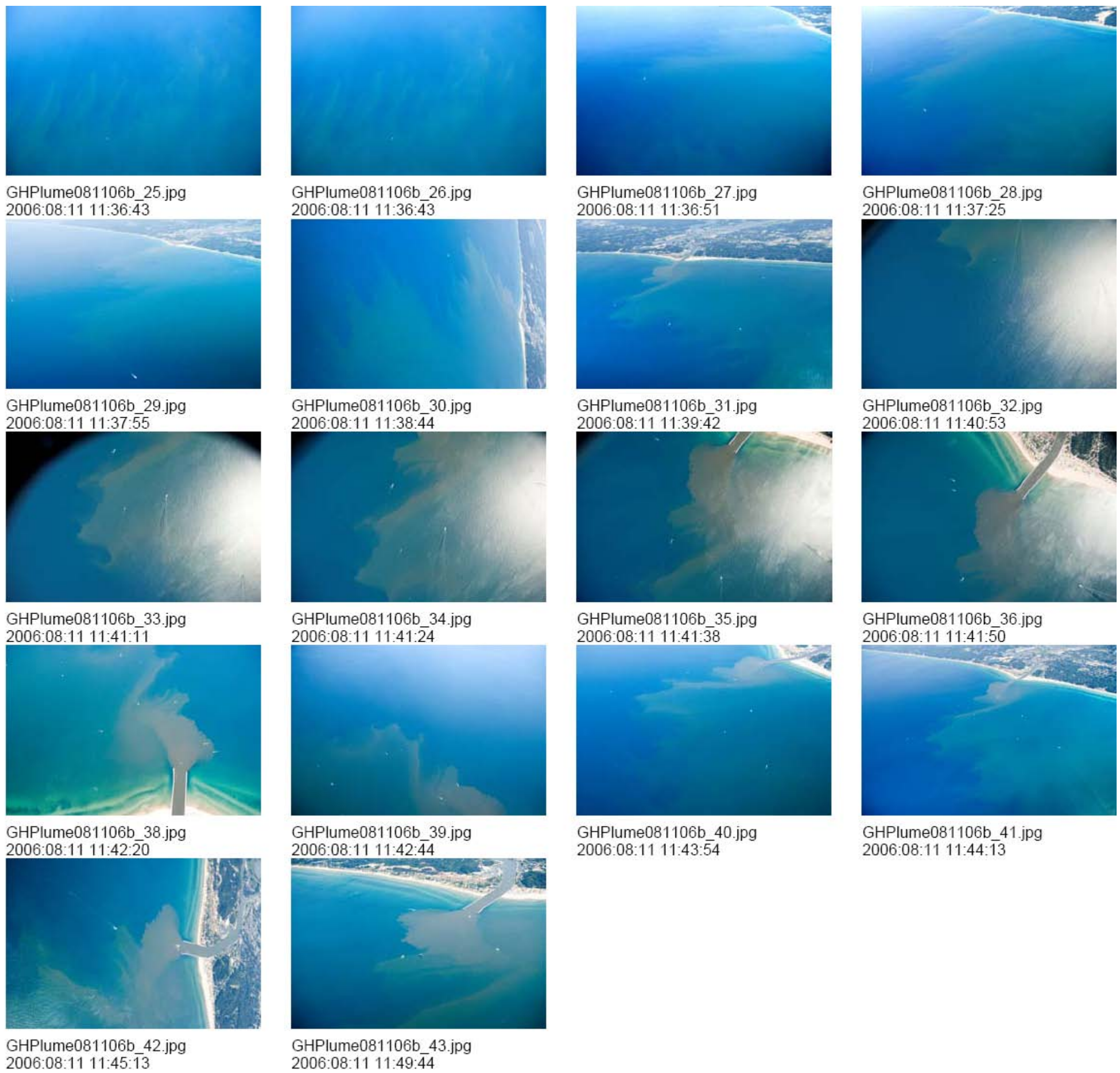

Figure A.9. Aerial pictures of the Grand Haven Plume on August 11, 2006 from 11:36:43 to 11:49:44 EDT.

A.3. May 2007

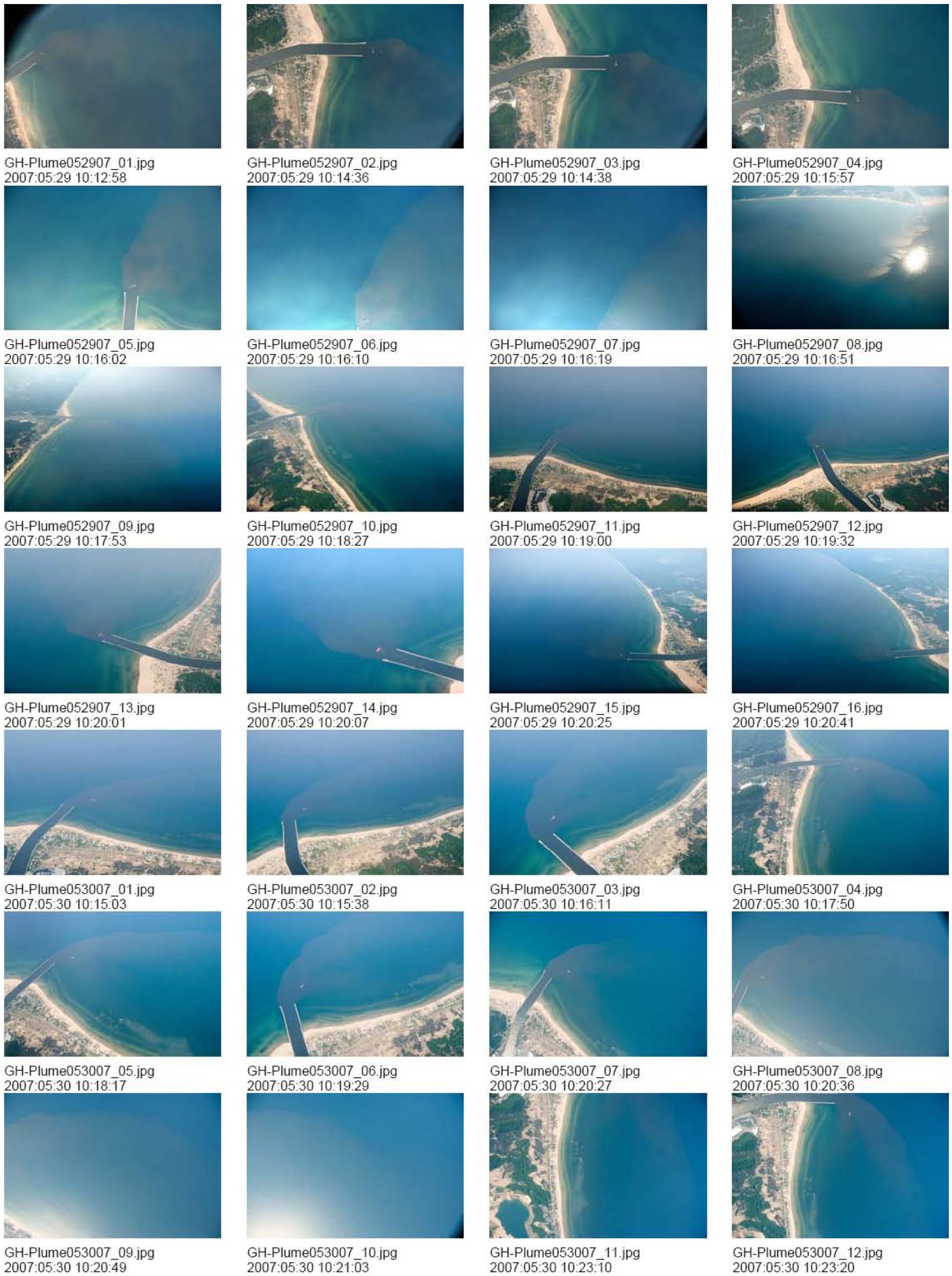

Figure A.10. Aerial pictures of the Grand Haven Plume from May 29, 2007 10:12:58 EDT to May 30, 2007 10:23:20 EDT.

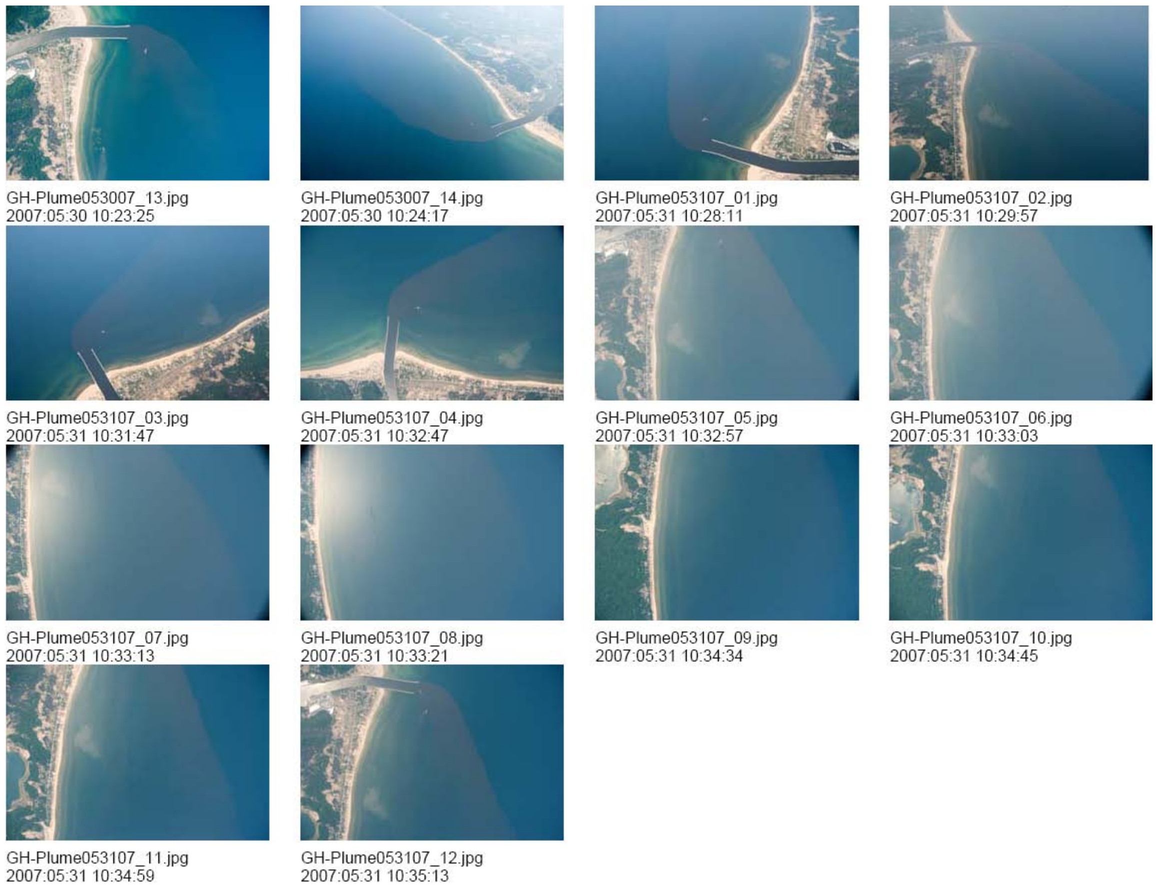

Figure A.11. Aerial pictures of the Grand Haven Plume during May 30, 2007 10:23:25 EDT to May 31, 2007 10:35:13 EDT.

A.4. June 2007

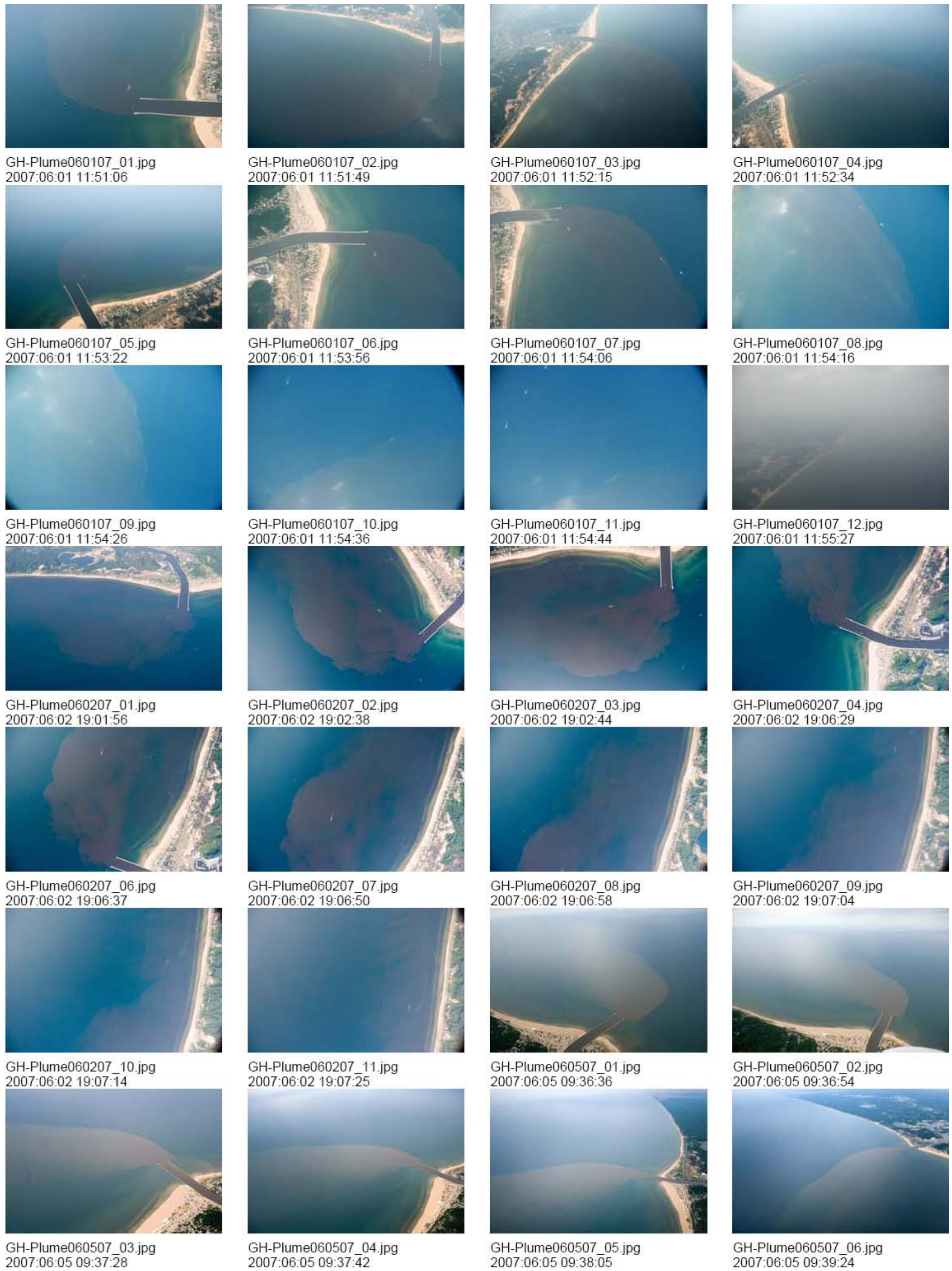

Figure A.12. Aerial pictures of the Grand Haven Plume from June 1, 2007 11:51:06 EDT to June 5, 2007 09:39:24 EDT.

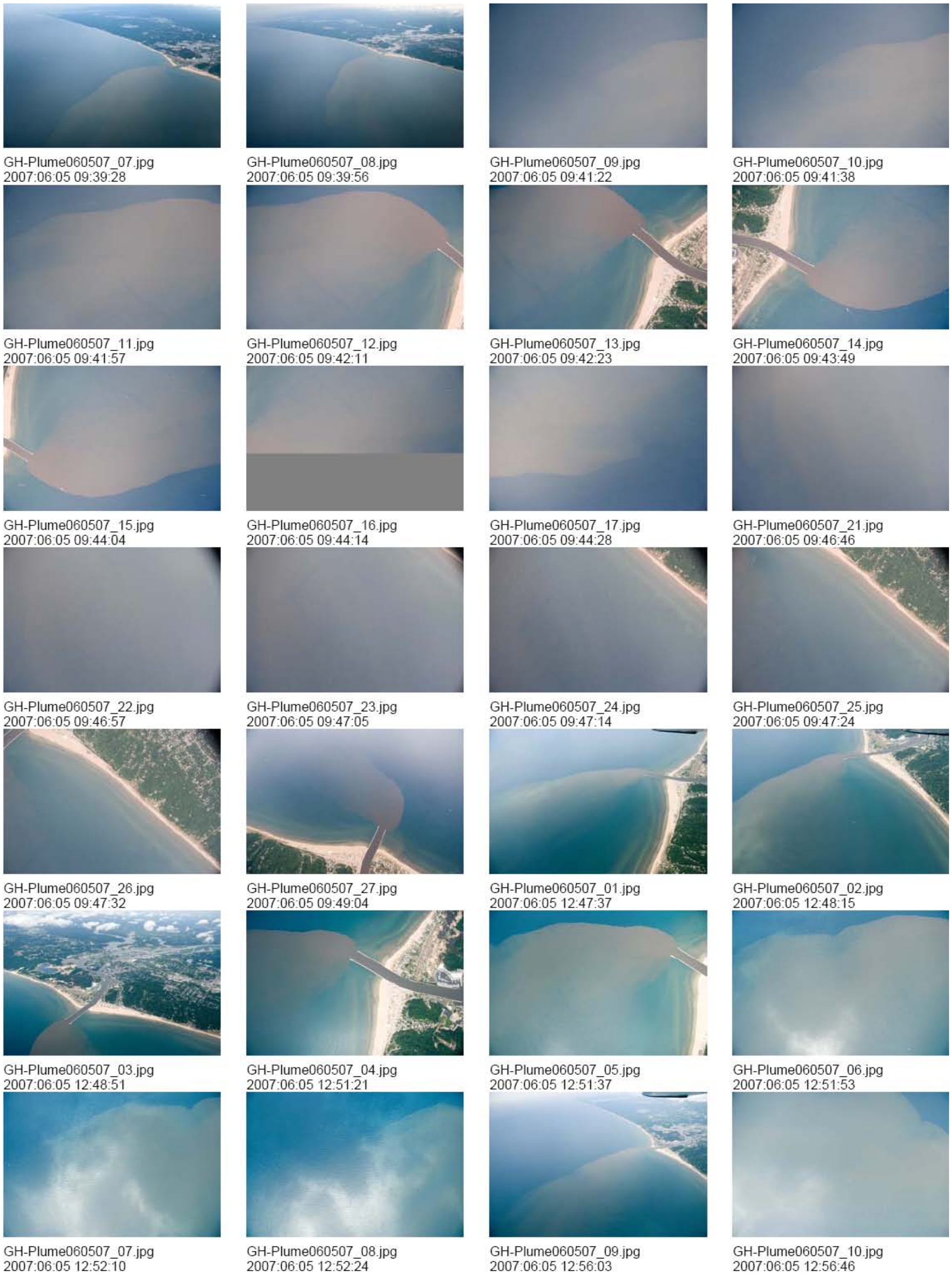

Figure A.13. Aerial pictures of the Grand Haven Plume on June 5, 2007, from 09:39:28 to 12:56:46 EDT.

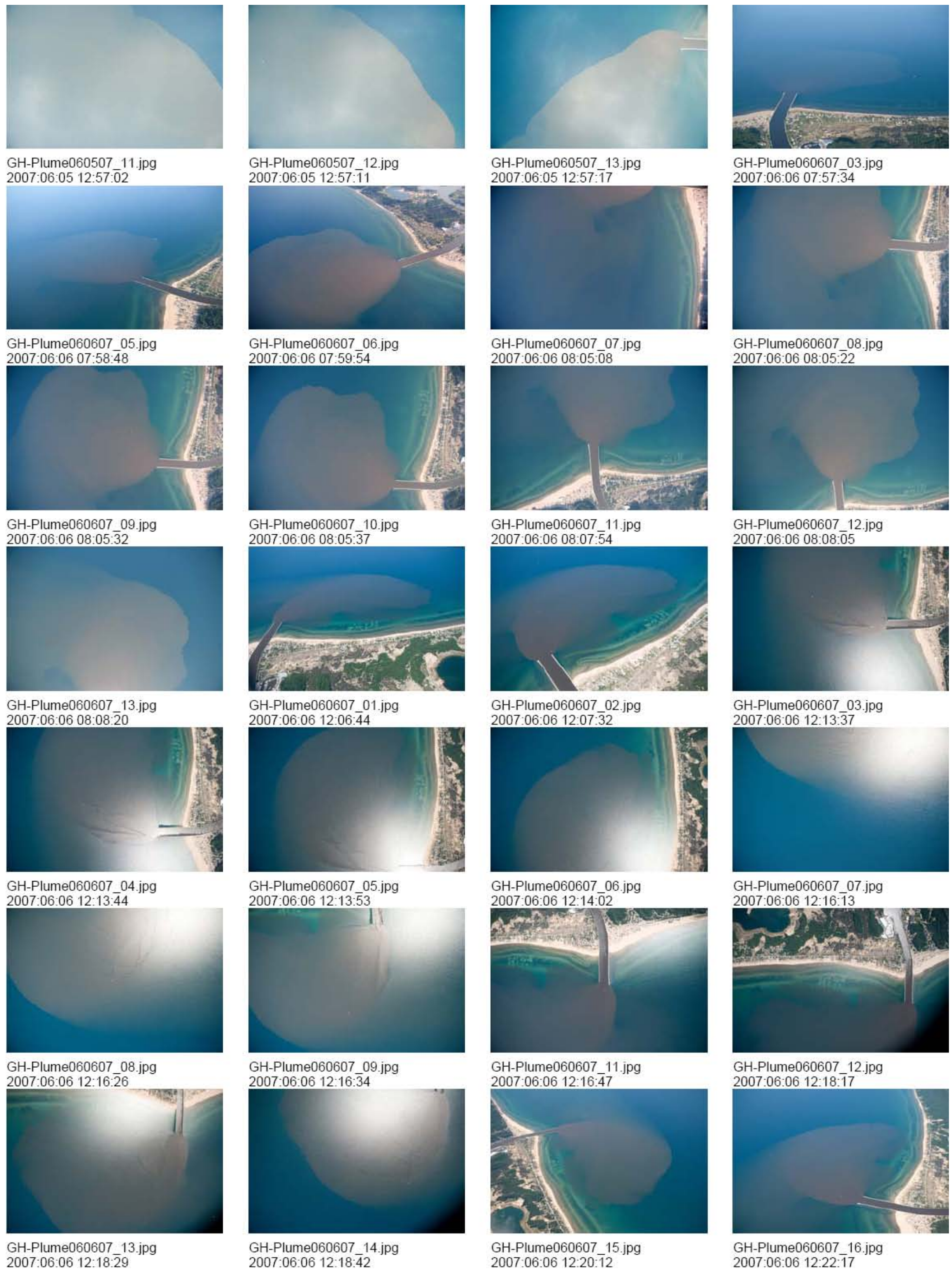

Figure A.14. Aerial pictures of the Grand Haven Plume from June 5, 2007 12:57:02 to June 6, 2007 12:22:17 EDT.

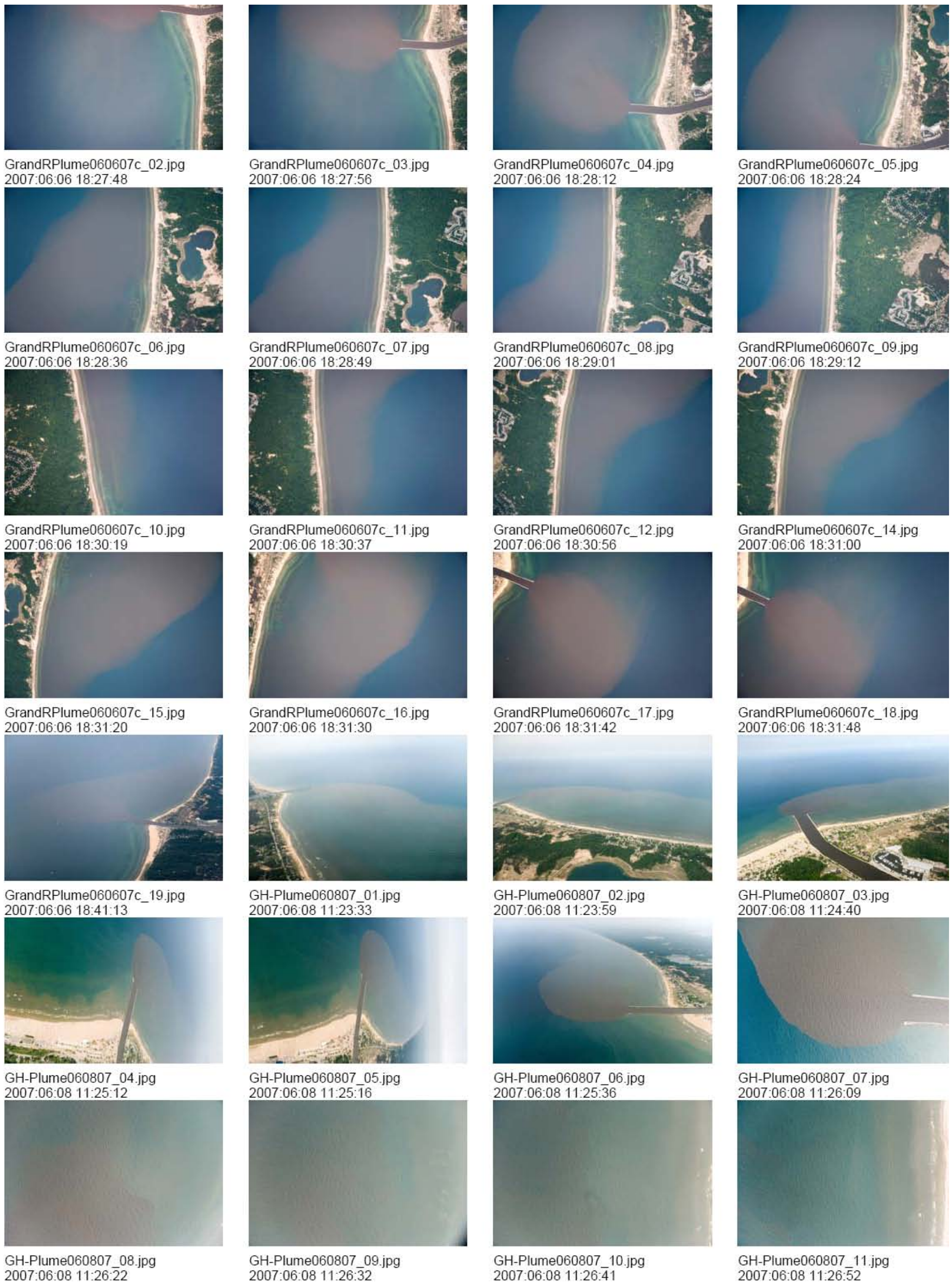

Figure A.15. Aerial pictures of the Grand Haven Plume from June 6, 2007, 18:27:48 to June 8, 2007, 11:26:52 EDT.

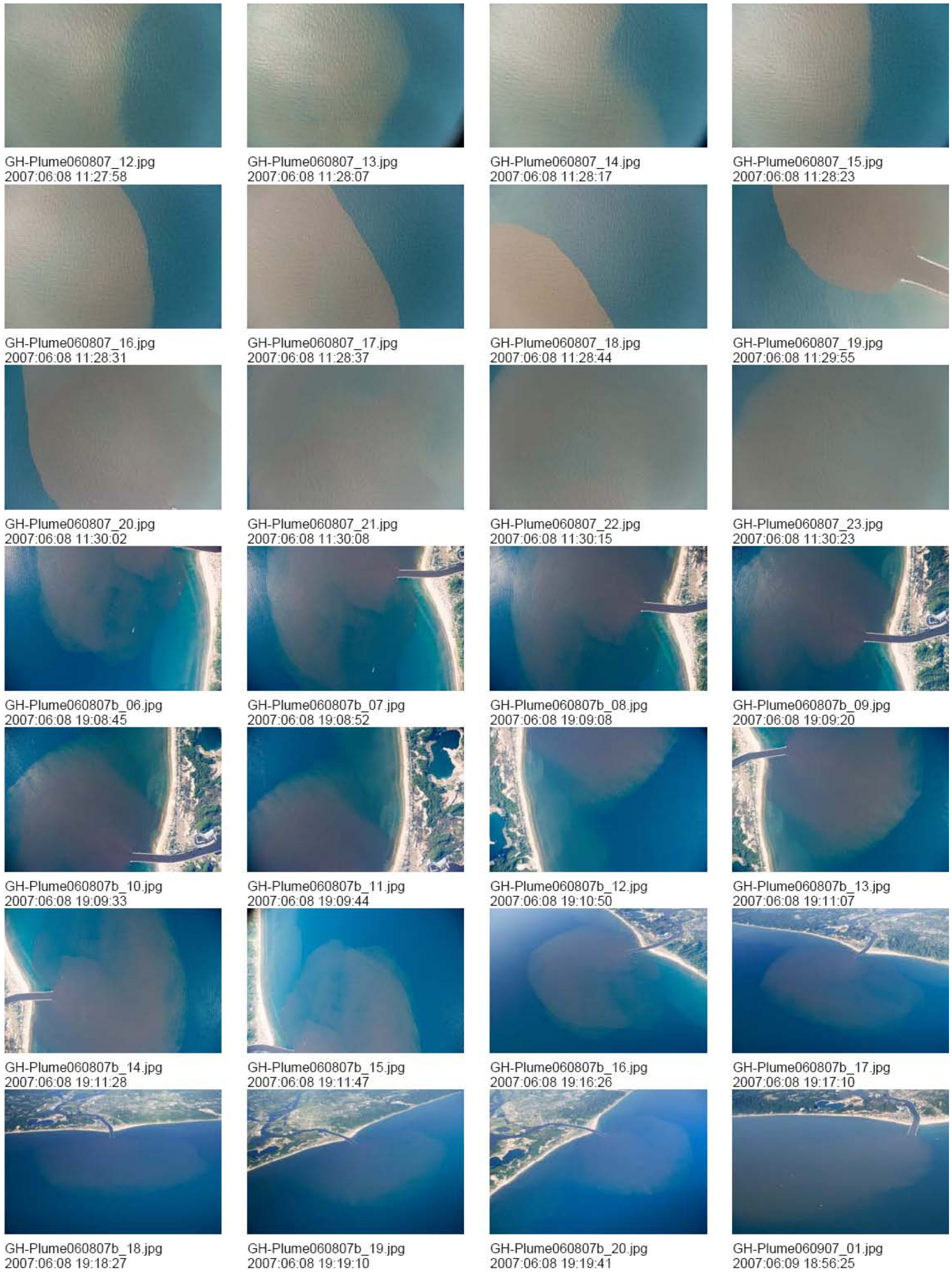

Figure A.16. Aerial pictures of the Grand Haven Plume from June 8, 2007, 11:27:58 to June 9, 2007, 18:56:25 EDT.

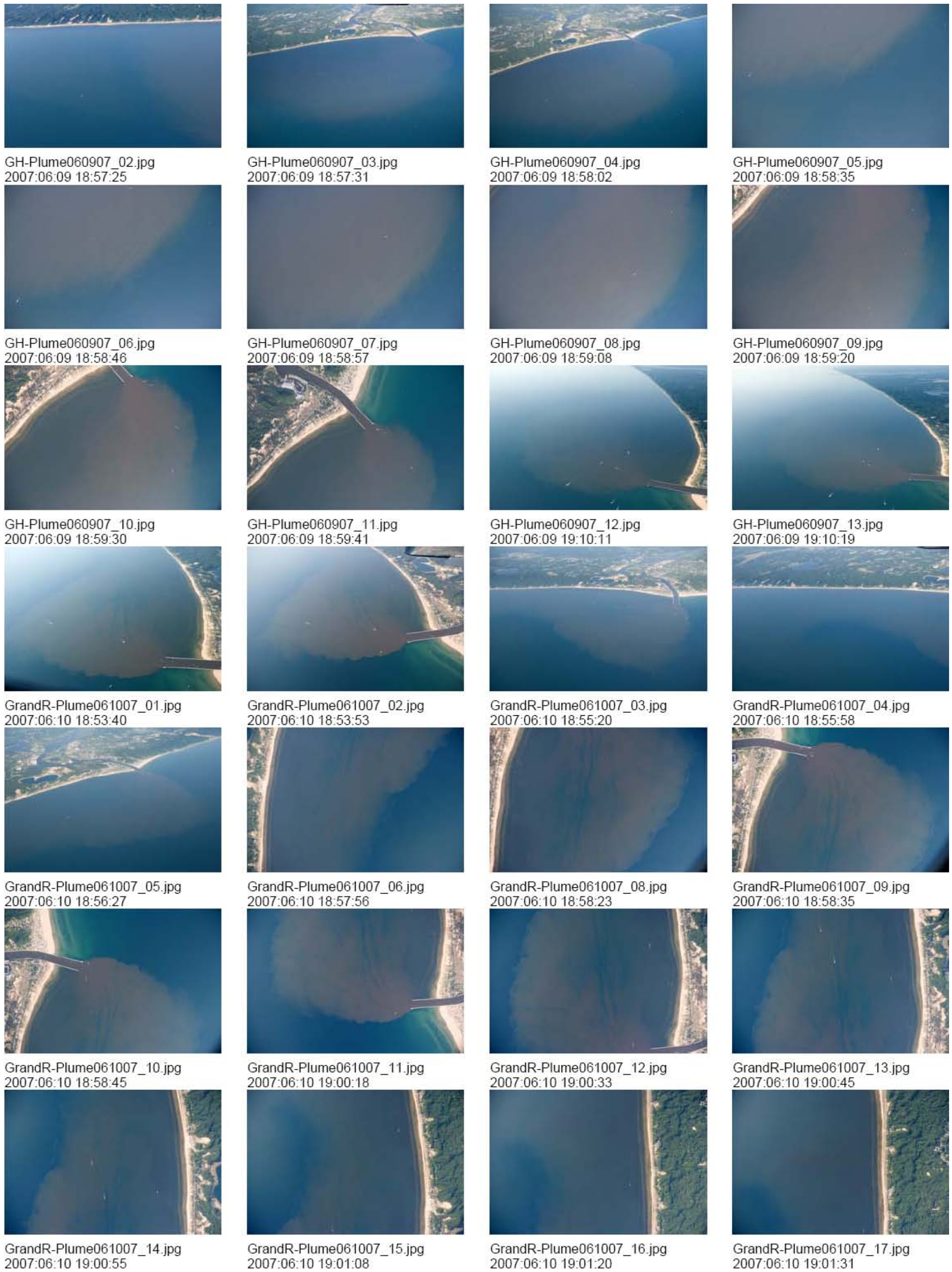

Figure A.17. Aerial pictures of the Grand Haven Plume on June 9, 2007, from 18:57:25 to June 10, 2007, 19:01:31 EDT.

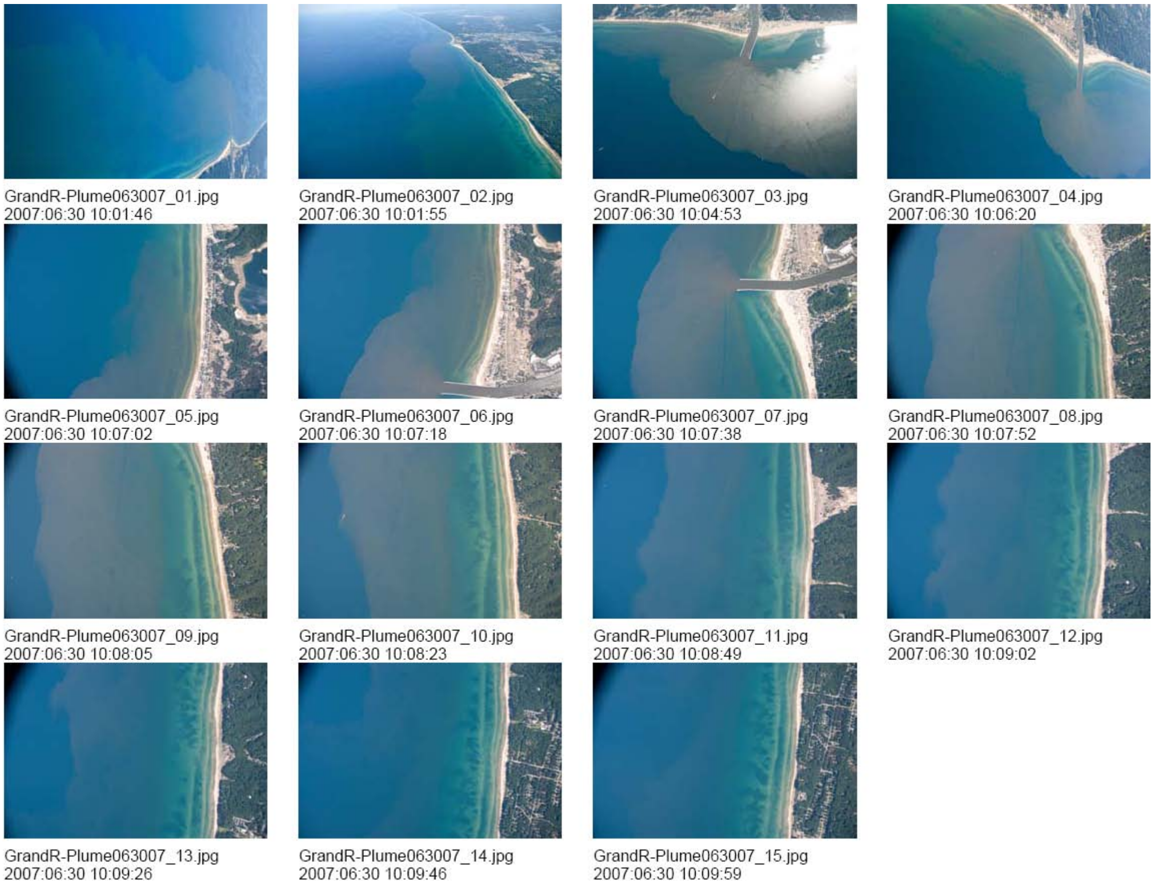

Figure A.18. Aerial pictures of the Grand Haven Plume on June 30, 2007, from 10:01:46 to 10:09:59 EDT.

A.5. July 2007

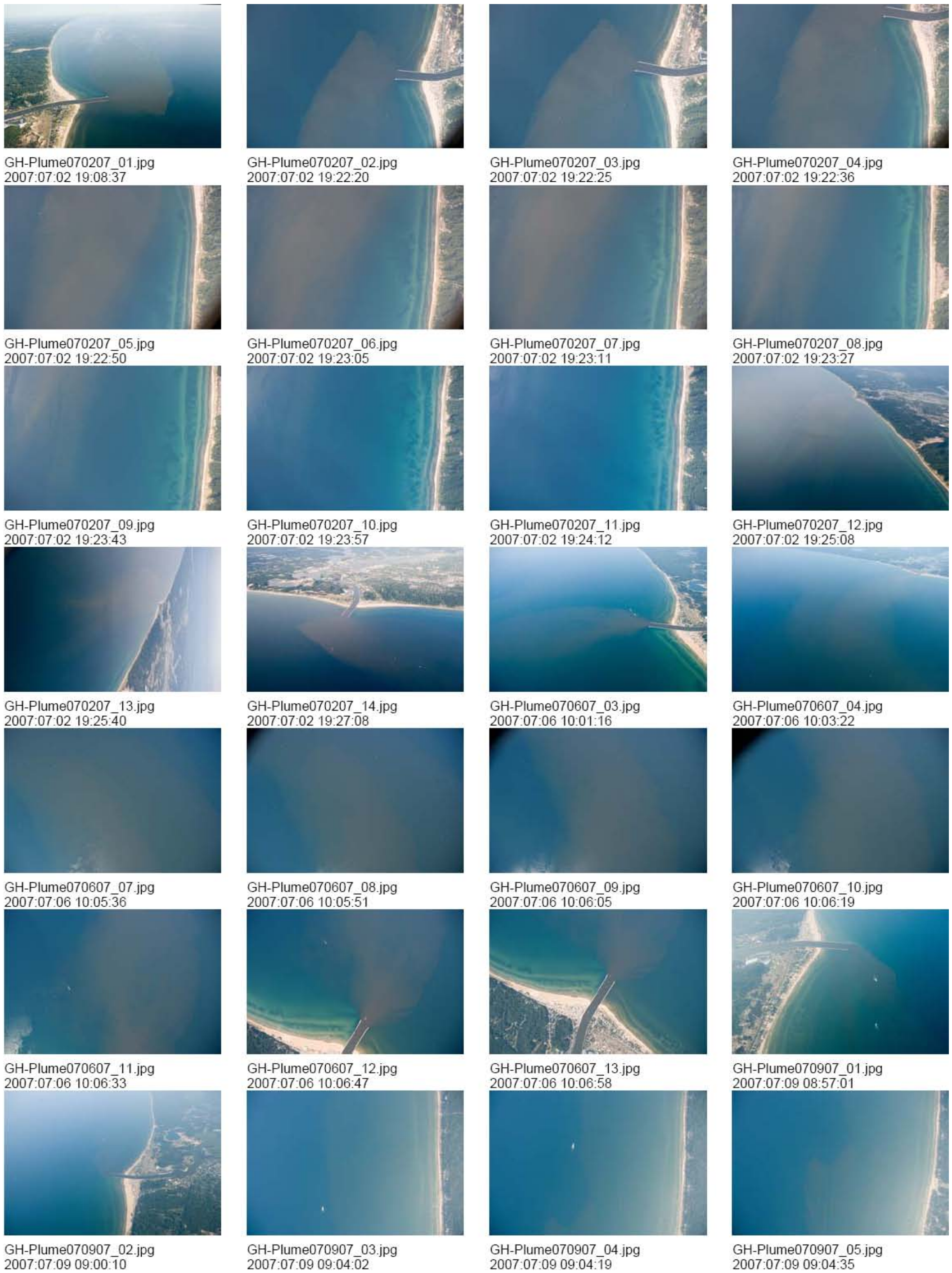

Figure A.19. Aerial pictures of the Grand Haven Plume from July 2, 2007, 19:08:37 to July 9, 2007, 09:04:35 EDT.

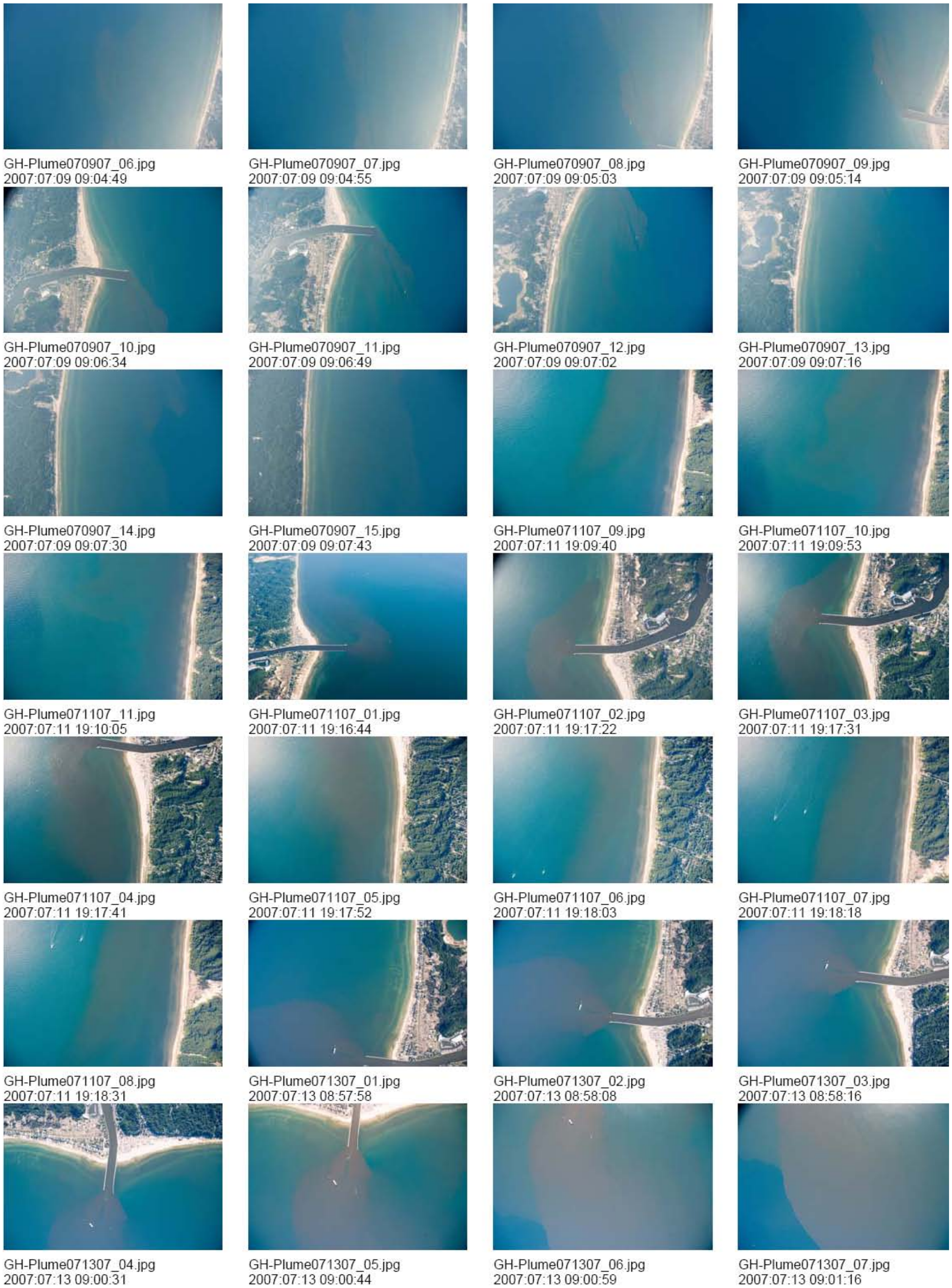

Figure A.20. Aerial pictures of the Grand Haven Plume from July 9, 2007, 09:04:49 to July 13, 2007, 09:01:16 EDT.

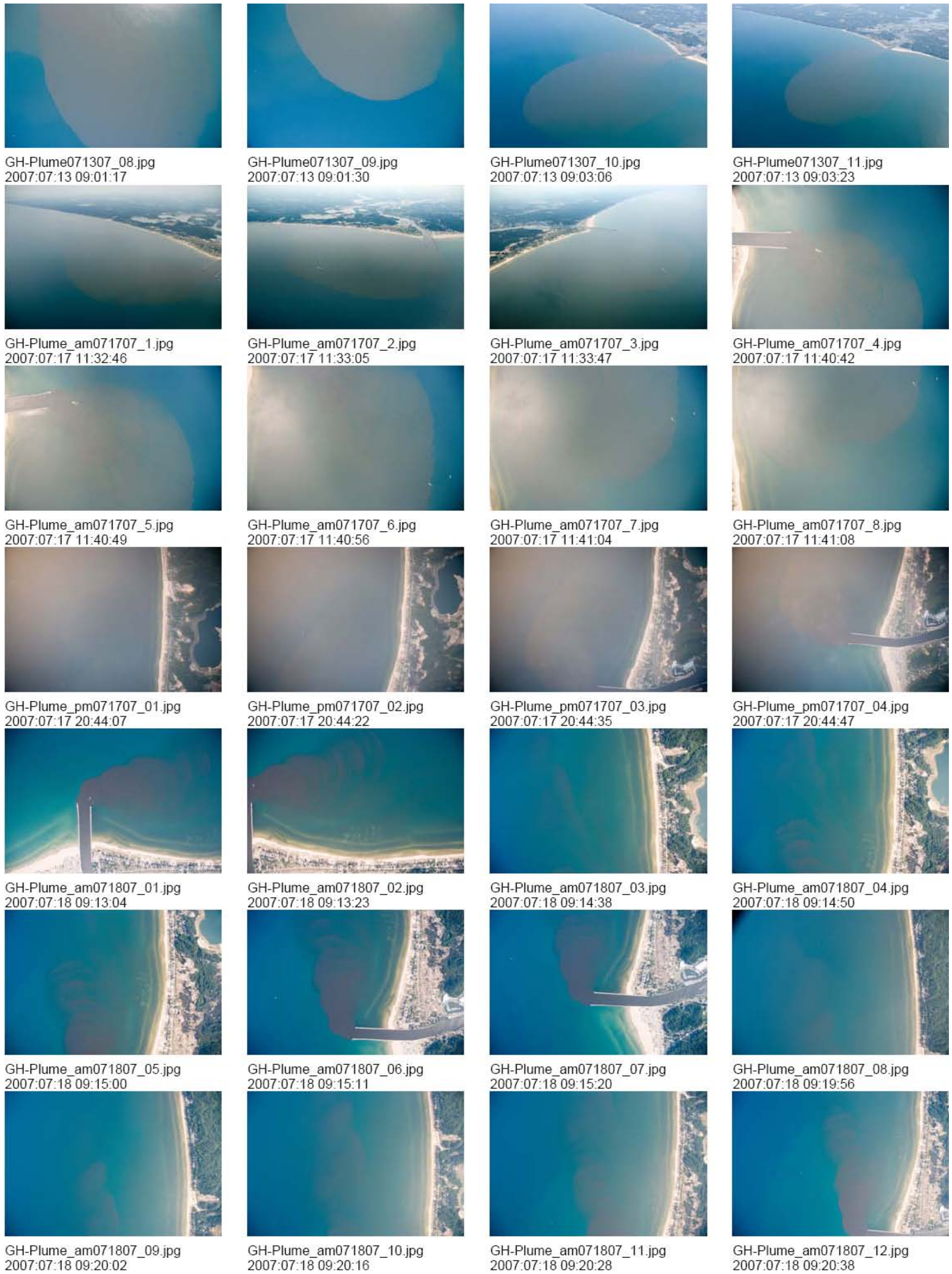

Figure A.21. Aerial pictures of the Grand Haven Plume from July 13, 2007 09:01:17 to July 18, 2007 09:20:38 EDT.

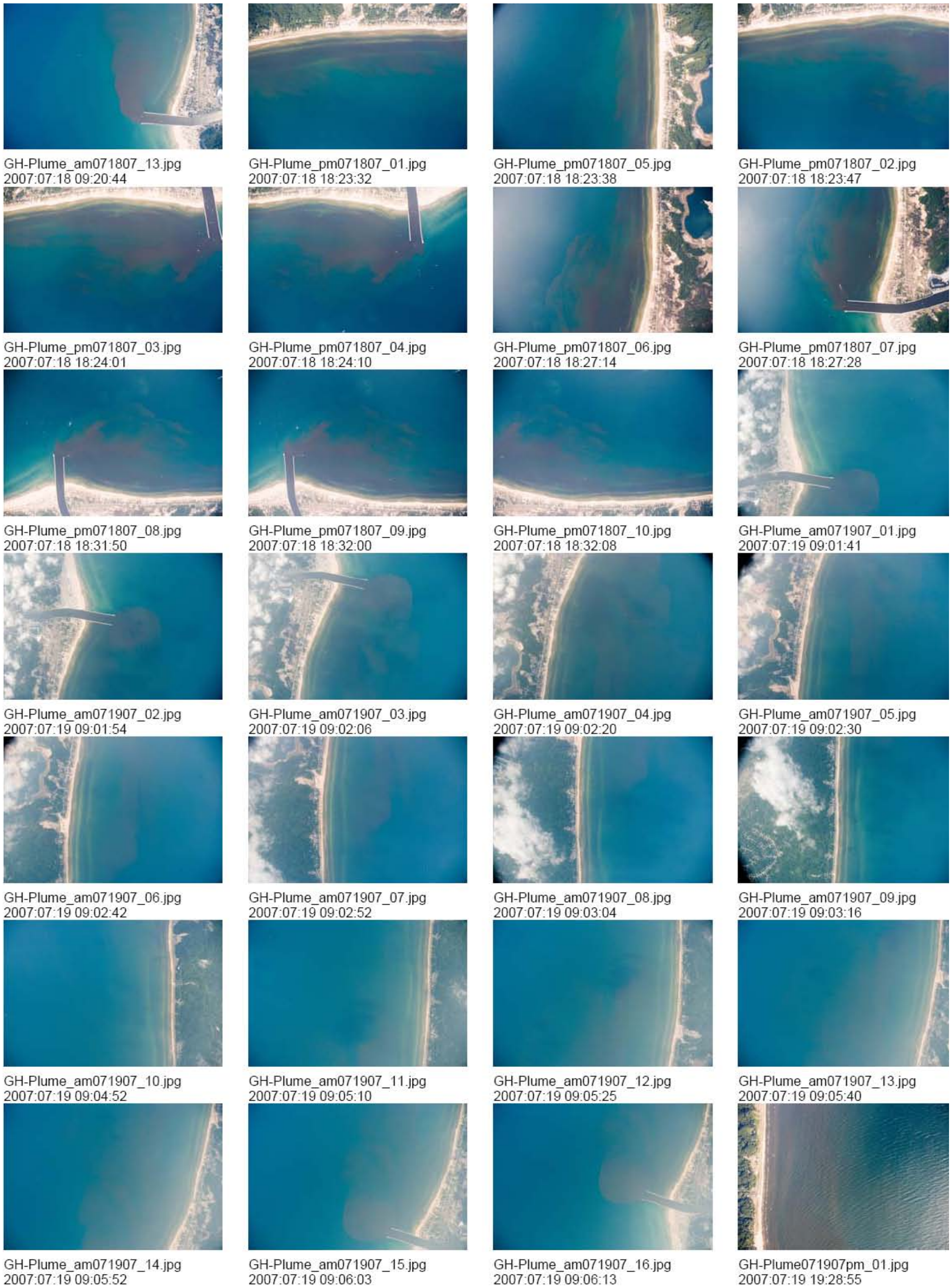

Figure A.22. Aerial pictures of the Grand Haven Plume from July 18, 2007, 09:20:44 to July 19, 2007 19:28:55 EDT.

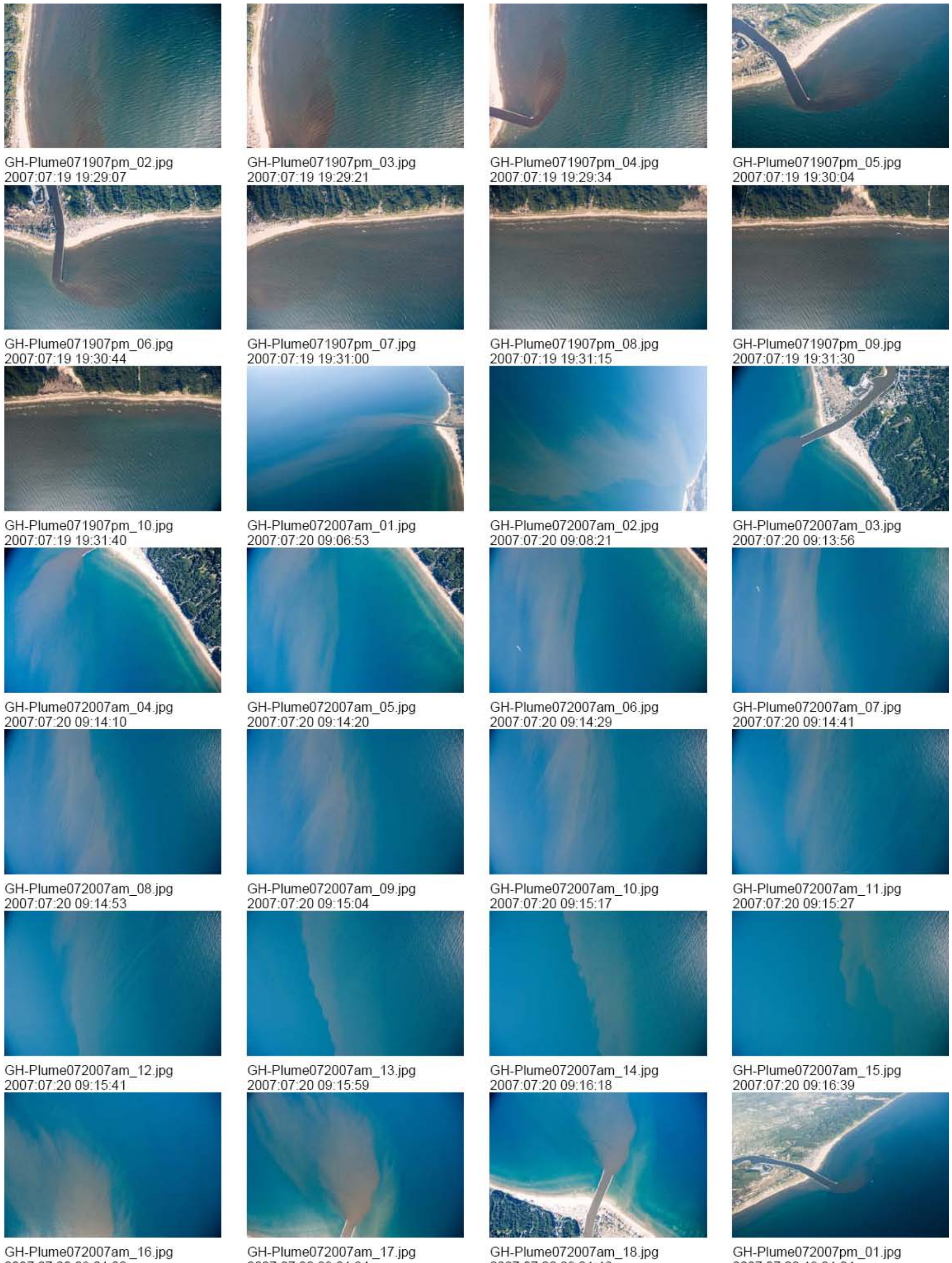

Figure A.23. Aerial pictures of the Grand Haven Plume from July 19, 2007, 19:29:07 to July 20, 2007 19:21:04 EDT.

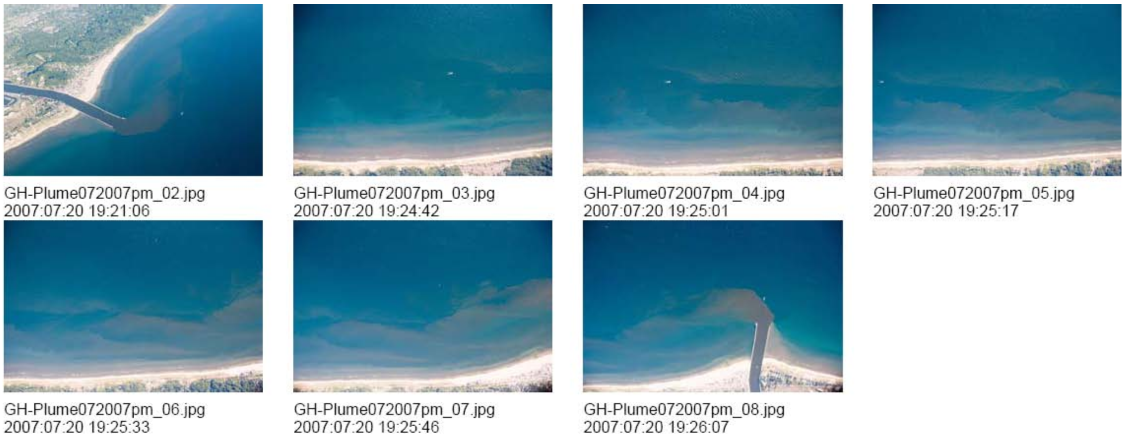

Figure A.24. Aerial pictures of the Grand Haven Plume on July 20, 2007, from 19:21:06 to 19:26:07 EDT.

APPENDIX B: POM GOVERNING EQUATIONS

The incompressibility, hydrostatic, and Buossinesq assumptions made in POM are as follows:

$$\frac{D\rho}{Dt} = 0 \tag{B-1}$$

$$P(x,y,z) = P_{atm} + g\rho_{\circ}\eta + g\int_{z}^{0} \rho(x,y,z',t)dz' \tag{B-2}$$

$$\frac{\partial P}{\partial x} = \frac{\partial P_{atm}}{\partial x} + \rho_{\circ} g\frac{\partial \eta}{\partial x} + \int_{z}^{0} \frac{g}{\rho_{\circ}}\frac{\partial P}{\partial x}dz \tag{B-3}$$

$$\frac{1}{\rho}\frac{\partial P}{\partial x} = g\frac{\partial \eta}{\partial x} + \int \frac{g}{\rho_{\circ}}\frac{\partial P}{\partial x}dz \tag{B-4}$$

Basic equations of continuity, momentum, and thermodynamics including temperature and salinity in Cartesian coordinates are described are as follows:

$$\nabla \cdot \bar{V} + \frac{\partial W}{\partial z} = 0 \tag{B-5}$$

$$\frac{\partial U}{\partial t} + \bar{V}\cdot\nabla U + W\frac{\partial U}{\partial z} - f\,V = -\frac{1}{\rho_0}\frac{\partial P}{\partial x} + \frac{\partial}{\partial z}\left(K_M \frac{\partial U}{\partial z}\right) + F_X \tag{B-6}$$

$$\frac{\partial V}{\partial t} + \bar{V}\cdot\nabla V + W\frac{\partial V}{\partial z} - f\,U = -\frac{1}{\rho_0}\frac{\partial P}{\partial y} + \frac{\partial}{\partial z}\left(K_M \frac{\partial V}{\partial z}\right) + F_Y \tag{B-7}$$

$$\frac{\partial \theta}{\partial t} + \bar{V}\cdot\nabla\theta + W\frac{\partial \theta}{\partial z} = \frac{\partial}{\partial z}\left(K_H\frac{\partial \theta}{\partial z}\right) + F_{\theta} \tag{B-8}$$

$$\frac{\partial S}{\partial t} + \bar{V}\cdot\nabla S + W\frac{\partial S}{\partial z} = \frac{\partial}{\partial z}\left(K_H\frac{\partial S}{\partial z}\right) + F_{S} \tag{B-9}$$

The equation of state (Mellor, 1991) calculates the density as a function of temperature, salinity, and pressure:

$$\rho = \rho(\theta, S, p) \tag{B-10}$$

where θ, and S are respectively the potential temperature and salinity, U , V , W are the velocity vectors in *x*, *y*, and *z* directions, *p* is the pressure, *f* is the Coriolis term, K_H is the heat/salt vertical eddy diffusivity and K_M is the momentum vertical eddy diffusivity.

F_x , F_y , and $F_{\theta,S}$ are the horizontal viscosity terms. The horizontal viscosity and diffusion terms are:

$$F_x = \frac{\partial}{\partial x}\left[2A_M \frac{\partial U}{\partial x}\right] + \frac{\partial}{\partial y}\left[A_M\left(\frac{\partial U}{\partial y} + \frac{\partial V}{\partial x}\right)\right] \tag{B-11}$$

$$F_y = \frac{\partial}{\partial y}\left[2A_M \frac{\partial V}{\partial y}\right] + \frac{\partial}{\partial x}\left[A_M\left(\frac{\partial U}{\partial y} + \frac{\partial V}{\partial x}\right)\right] \tag{B-12}$$

$$F_{\theta,S} = \frac{\partial}{\partial x}\left[2A_M \frac{\partial(\theta,S)}{\partial x}\right] + \frac{\partial}{\partial y}\left[A_H \frac{\partial(\theta,S)}{\partial x}\right] \tag{B-13}$$

$$A_M = C\Delta x\Delta y\frac{1}{2}\left|\nabla V + \left(\nabla V\right)^T\right| \tag{B-14}$$

where A_M (the same as K_h in PARTIC3D), and A_H are horizontal eddy diffusivities that damp small-scale computational noise. Horizontal momentum diffusion is assumed to be equal to horizontal thermal diffusion where the primary mixing process is eddy diffusion. The Smagorinsky diffusivity, A_M, is small for computations with high resolution and small velocity gradient.

The model includes the Mellor and Yamada (1982) level 2.5 turbulence closure parameterization.

$$\frac{\partial q^2}{\partial x} + \vec{V}\cdot\nabla q^2 + W\frac{\partial q^2}{\partial z} =$$

$$\frac{\partial}{\partial z}\left(K_q\frac{\partial q^2}{\partial z}\right) + 2K_M\left(\left(\frac{\partial U}{\partial z}\right)^2 + \left(\frac{\partial V}{\partial z}\right)^2\right) + \frac{2g}{\rho_\circ}K_H\frac{\partial \rho}{\partial x} - \frac{2q^3}{B_1 l} + F_q \tag{B-15}$$

and

$$\frac{\partial\left(q^2\ell\right)}{\partial t} + \vec{V}\cdot\nabla\left(q^2\ell\right) + W\frac{\partial\left(q^2\ell\right)}{\partial z} =$$

$$\frac{\partial}{\partial z}\left(K_q\frac{\partial\left(q^2\ell\right)}{\partial z}\right) + \ell E_1 K_M\left(\left(\frac{\partial U}{\partial z}\right)^2 + \left(\frac{\partial V}{\partial z}\right)^2\right) + \frac{\ell E_1 g}{\rho_\circ}K_H\frac{\partial \rho}{\partial z} - \frac{q^3}{B_1}\tilde{W} + F_\ell \tag{B-16}$$

where

$$K_M \equiv \ell q S_M, \qquad K_H \equiv \ell q S_H, \qquad K_q \equiv \ell q S_q \tag{B-17}$$

and K_M, K_H (the same as K_v in PARTIC3D), and K_q are the turbulence mixing coefficients, and S_M, S_H, and S_q are the analytical stability functions, ℓ is the turbulence macroscale, q is the turbulence kinetic energy, F_q and F_l are horizontal turbulence mixing terms, and, B_1 and E_1 are empirical constants (refer to Blumberg and Mellor, 1987 for further detail).

The above basic equations are given in a horizontal Cartesian z-coordinate system. In terms of grids, horizontal orthogonal-curvilinear coordinates and Cartesian are easily implemented. In POM Sigma vertical coordinates (important for varying topography) are also included (Figure B.1).

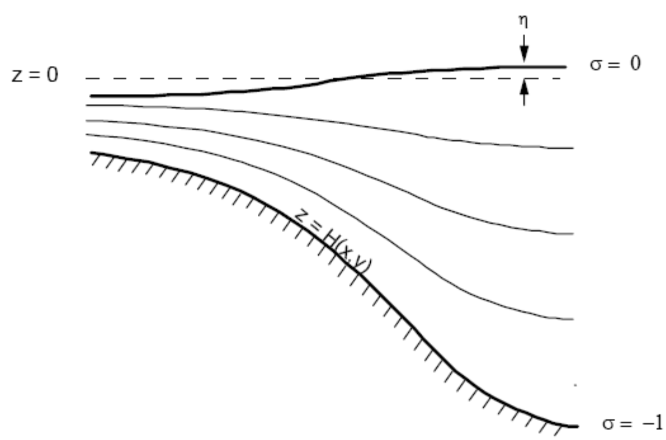

Figure B.1. Sigma Coordinates.

The transformed equations after applying sigma level coordinates are below.

$$x^* = x, \quad y^* = y, \quad \sigma = \frac{z-\eta}{H+\eta}, \quad t^* = t \tag{B-18}$$

$$\frac{\partial DU}{\partial x} + \frac{\partial DV}{\partial y} + \frac{\partial \omega}{\partial \sigma} + \frac{\partial \eta}{\partial t} = 0 \tag{B-19}$$

$$\begin{aligned} &\frac{\partial UD}{\partial t} + \frac{\partial U^2 D}{\partial x} + \frac{\partial UVD}{\partial y} + \frac{\partial U\omega}{\partial \sigma} - f\,VD + gD\frac{\partial \eta}{\partial x} + \\ &\quad \frac{gD^2}{\rho_\circ}\int_\sigma^0 \left[\frac{\partial \rho'}{\partial x} - \frac{\sigma'}{D}\frac{\partial D}{\partial x}\frac{\partial \rho'}{\partial \sigma'}\right] d\sigma' = \frac{\partial}{\partial \sigma}\left[\frac{K_M}{D}\frac{\partial U}{\partial \sigma}\right] + F_x \end{aligned} \tag{B-20}$$

$$\frac{\partial VD}{\partial t} + \frac{\partial UVD}{\partial x} + \frac{\partial V^2 D}{\partial y} + \frac{\partial V\omega}{\partial \sigma} + f\,UD + gD\frac{\partial \eta}{\partial y} + \frac{gD^2}{\rho_\circ}\int_\sigma^0 \left[\frac{\partial \rho'}{\partial y} - \frac{\sigma'}{D}\frac{\partial D}{\partial y}\frac{\partial \rho'}{\partial \sigma'}\right] d\sigma' = \frac{\partial}{\partial \sigma}\left[\frac{K_M}{D}\frac{\partial V}{\partial \sigma}\right] + F_y \tag{B-21}$$

$$\frac{\partial TD}{\partial t} + \frac{\partial TUD}{\partial x} + \frac{\partial TVD}{\partial y} + \frac{\partial T\omega}{\partial \sigma} = \frac{\partial}{\partial \sigma}\left[\frac{K_H}{D}\frac{\partial T}{\partial \sigma}\right] + F_T - \frac{\partial R}{\partial z} \tag{B-22}$$

$$\frac{\partial SD}{\partial t} + \frac{\partial SUD}{\partial x} + \frac{\partial SVD}{\partial y} + \frac{\partial S\omega}{\partial \sigma} = \frac{\partial}{\partial \sigma}\left[\frac{K_H}{D}\frac{\partial S}{\partial \sigma}\right] + F_S \tag{B-23}$$

$$\frac{\partial q^2 D}{\partial t} + \frac{\partial Uq^2 D}{\partial x} + \frac{\partial Vq^2 D}{\partial y} + \frac{\partial \omega q^2}{\partial \sigma} = \frac{\partial}{\partial \sigma}\left(\frac{K_q}{D}\frac{\partial q^2}{\partial \sigma}\right) + \frac{2K_M}{D}\left(\left(\frac{\partial U}{\partial \sigma}\right)^2 + \left(\frac{\partial V}{\partial \sigma}\right)^2\right) + \frac{2g}{\rho_0}K_H\frac{\partial \tilde{\rho}}{\partial \sigma} - \frac{2Dq^3}{B_1 \ell} + F_q \tag{B-24}$$

$$\frac{\partial q^2 \ell D}{\partial t} + \frac{\partial Uq^2 \ell D}{\partial x} + \frac{\partial Vq^2 \ell D}{\partial y} + \frac{\partial \omega q^2 \ell}{\partial \sigma} = \frac{\partial}{\partial \sigma}\left(\frac{K_q}{D}\frac{\partial q^2 \ell}{\partial \sigma}\right) \tag{B-25}$$

$$W = \omega + U\left(\sigma\frac{\partial D}{\partial x} + \frac{\partial \eta}{\partial x}\right) + V\left(\sigma\frac{\partial D}{\partial y} + \frac{\partial \eta}{\partial y}\right) + \sigma\frac{\partial D}{\partial t} + \frac{\partial \eta}{\partial t} \tag{B-26}$$

$$F_x = \frac{\partial}{\partial x}\left[H\tau_{xx}\right] + \frac{\partial}{\partial y}\left[H\tau_{yy}\right] \tag{B-27}$$

$$A_M = C\Delta x\Delta y\frac{1}{2}\left[\left(\partial u/\partial x\right)^2 + \left(\partial v/\partial x + \partial u/\partial y\right)^2/2 + \left(\partial v/\partial y\right)^2\right]^{1/2} \tag{B-28}$$

APPENDIX C: POMGL SENSITIVITY ANALYSIS

Bottom roughness was defined as an asymptotic function, $z_0 = a + b/(c+h)$. Below are the model sensitivity in response to variation of the parameters a, b, and c.

C.1. Effect of parameter a in roughness height on POMGL predictions

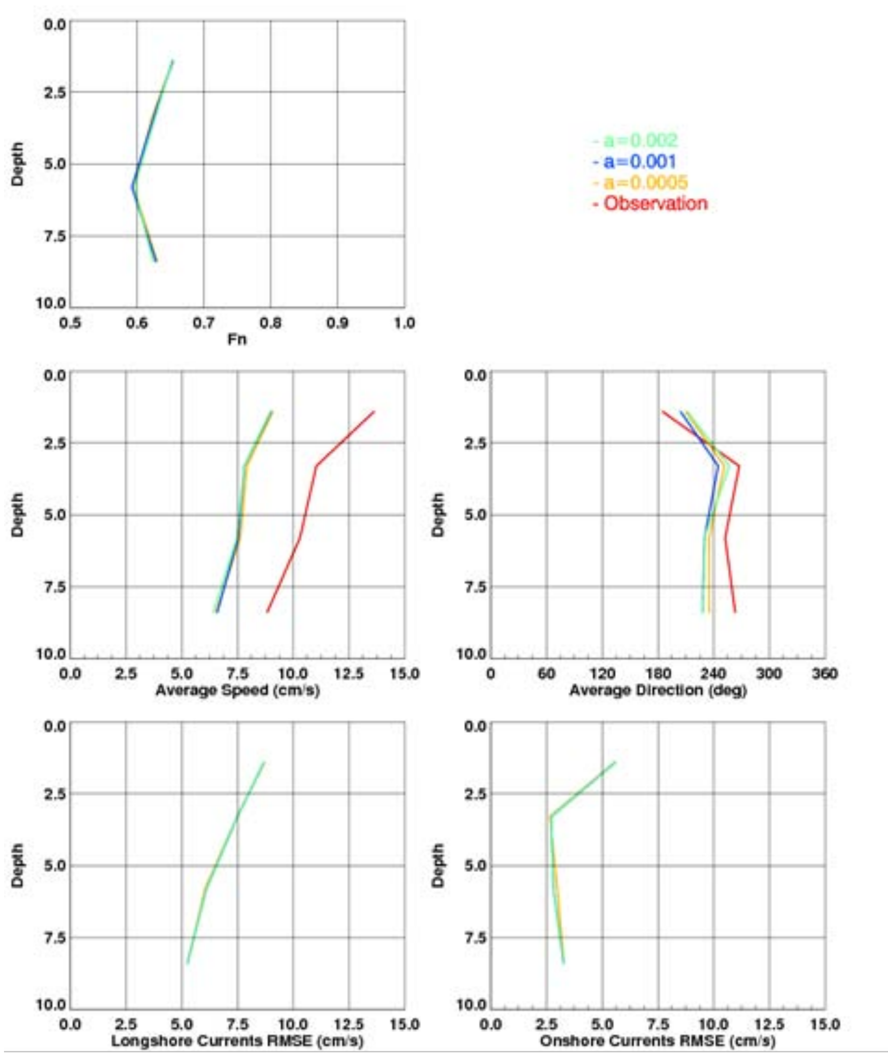

Figure 0.1 Effect of parameter a on Fourier Norm, average speed and direction, and longshore and onshore currents RMSE during June 19-24, 2006; observation is in red.

C.2. Effect of parameter b in roughness height on POMGL predictions

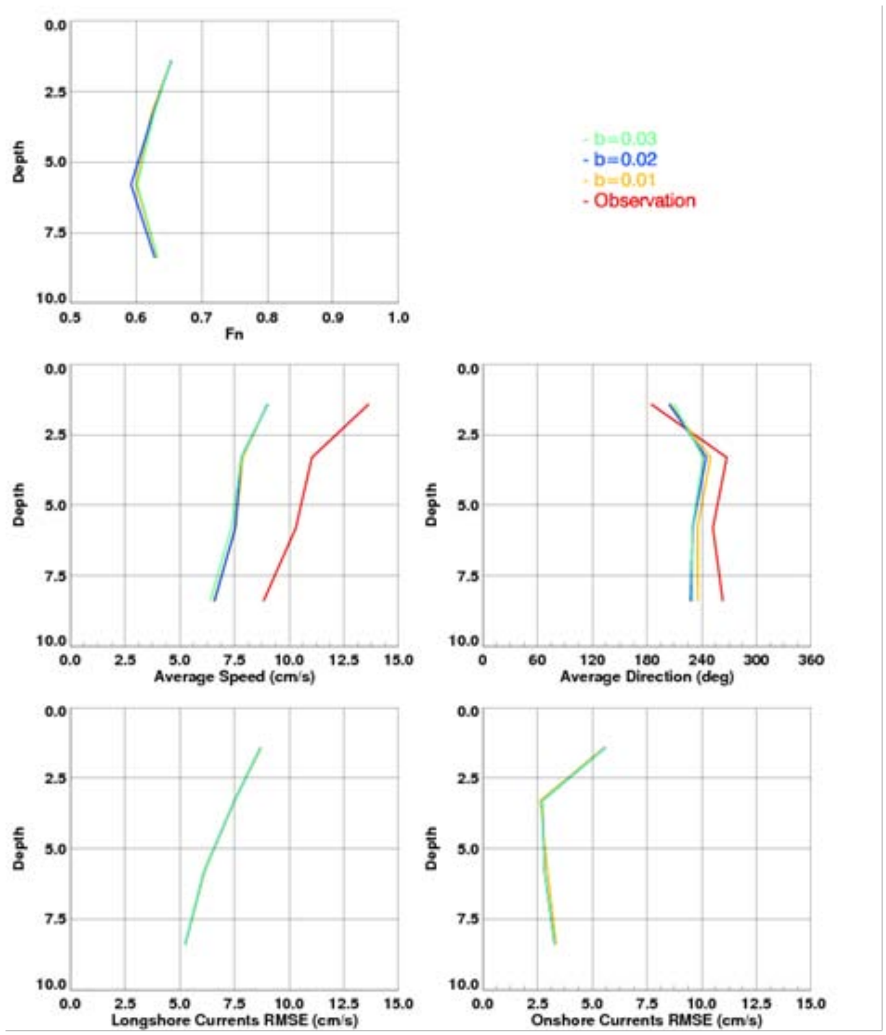

Figure 0.2 Effect of parameter b on Fourier Norm, average speed and direction, and longshore and onshore currents RMSE during June 19-24, 2006; observation is in red.

C.3. Effect of parameter c in roughness height on POMGL predictions

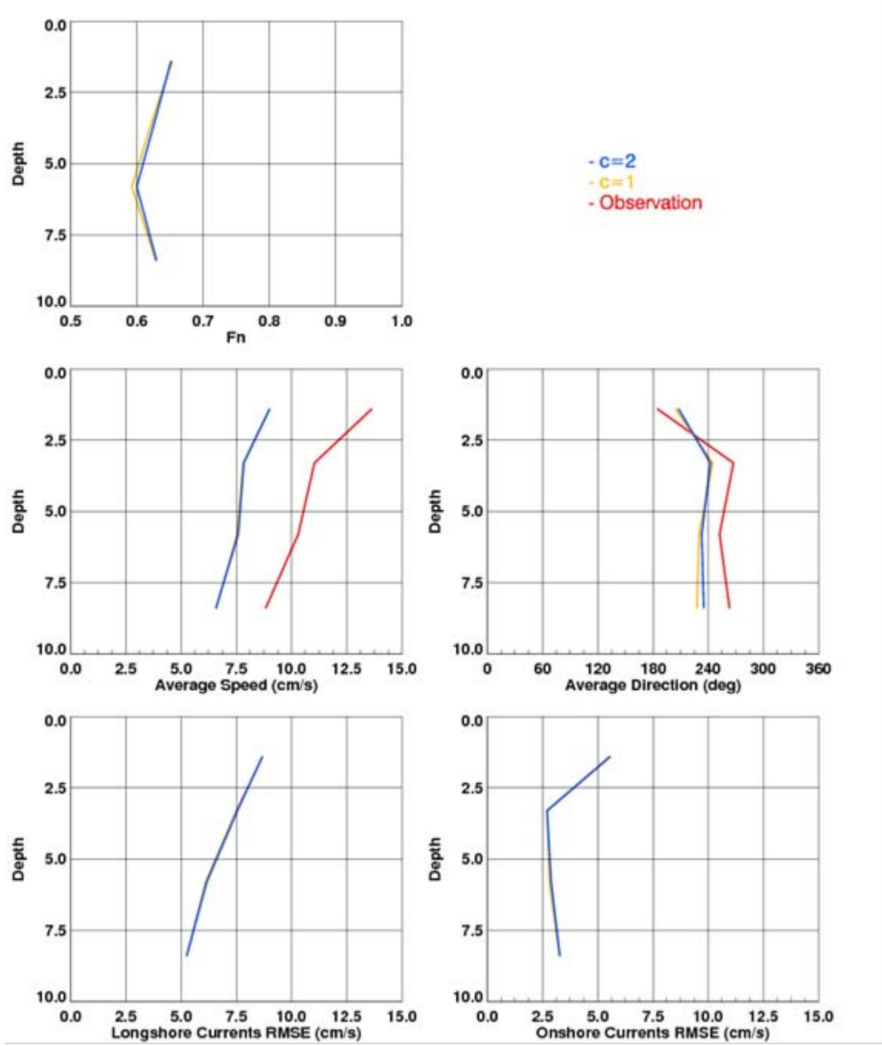

Figure C.3 Effect of parameter c on Fourier Norm, average speed and direction, and longshore and onshore currents RMSE during June 19-24, 2006; observation is in red.

Sensitivity of the model to horizontal diffusion is tested by changing the HORCON parameter in Smagorinsky eddy term. The results are shown below.

C.4. Effect of parameter HORCON (horizontal diffusion) on POMGL predictions

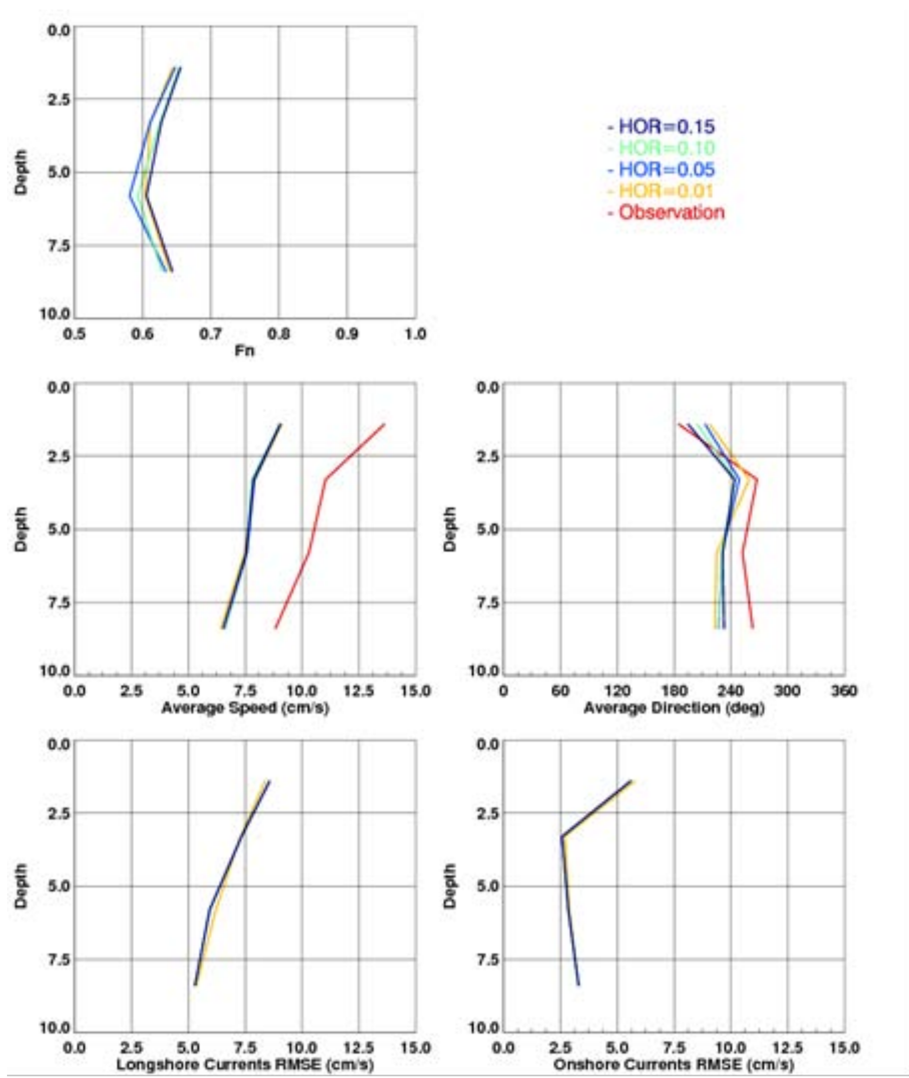

Figure 0.4 Effect of parameter HORCON on Fourier Norm, average speed and direction, and longshore and onshore currents RMSE during June 19-24, 2006; observation is in red.